PARTICLE PRODUCTION PROCESSES IN HIGH ENERGY PHYSICS

by

GORDON MURRAY FRASER

A Thesis presented for the
Degree of Doctor of Philosophy
of the University of London.

Department of Theoretical Physics,
Imperial College of Science and Technology,
London.

May, 1967

PREFACE

The work described in this thesis was carried out under the supervision of Professor P. T. Matthews F.R.S. between October 1964 and April 1967 in the Department of Physics, Imperial College, University of London.

Except where otherwise stated, the material contained herein is original and has not been previously presented for a degree in this or any other university.

The author is sincerely grateful to Professor Matthews for his constant attention, advice and encouragement, and indeed to to all members of the Theoretical Physics and High-Energy Nuclear Physics Departments for their help. He must express his thanks to Dr. Richard Roberts, with whom he collaborated during the execution of this work.

A Research Studentship from the Science Research Council (formerly the Department of Scientific and Industrial Research) is gratefully acknowledged.

"... Most theorists are not interested in analyzing experiments - they want to predict the universe from scratch in one step, and preferably without a computer."

"... All theorists should do some phenomenology occasionally to anchor them to earth, in the same spirit as St. Paul used to sew tents between epistles."

C. Lovelace, 1966

CONTENTS

ABSTRACT

A brief review of high-energy scattering dynamics is presented with particular reference to the comparison of the predictions made by the various models to observed behaviour in the laboratory.

The essential kinematics of single particle production processes are concisely listed. A thorough investigation is then conducted into the possible effects of diffraction scattering in these processes and using the three reactions $Kp \to K\pi p$, $\pi p \to \rho\pi p$, $\pi p \to \pi\pi p$ as examples, definite conclusions are drawn.

In order to make these conclusions more quantitative, extensive calculations are carried out using Regge Pole techniques for these production reactions. This improved model seems to give a fairly complete picture of the observed background spectrum. Comprehensive results are presented for the reaction $\pi N \to \pi\pi N$.

It is shown that multiperipheral processes have the same behaviour as those containing internal diffraction verteces, and so the Drell-Deck virtual diffraction mechanism cannot be responsible for the production of enhancements which could be mistaken for resonances.

INTRODUCTION

It is the purpose of this thesis to set up squarely some aspects of the phenomenology of high-energy particle production processes in strong interactions and to determine to what extent the standard techniques of high-energy physics are successful in describing such reactions. To this end the work is divided into three main sections.

The first section is a self-contained unit which presents a general survey of the methods currently employed in the analysis of scattering processes. There are four main ideas that are important in practice; Peripheralism, Regge Pole Theory, Group Theory and Unitarity. Their inter-relation and interplay with each other is far from clear, but it is often possible to assign a specific method of attack to each particular type of scattering process. The various experiments are considered in turn, and the contentions of the different models examined with a view to establishing the range of validity of each one.

The major portion of the thesis is concerned with explicit investigations and calculations for reactions having two particles in the initial state and three finally. Thus the second section commences with a scheme of notation for these calculations which is subsequently

used consistently, and goes on to list all the kinematics needed.

The first investigations deal with the role of elastic diffraction scattering in production processes. The number of apparent resonances seen in the spectra for high-energy scatterings has long been a source of anxiety and a constant embarrassment, and it was suggested that some of these effects might be due to some quite mundane mechanism, notably diffraction, rather than a genuine resonance. The calculations presented show conclusively that diffraction scattering cannot ever account for resonance-like enhancements, in contrast with the claim of several authors. It now appears that this simple mechanism is responsible for a continuous background spectrum of the final state particles.

The final section contains a completely general angular momentum analysis for single particle production, the participating particles being of arbitrary spin. This leads to a model for the background spectrum which leans heavily on Regge Pole Theory. Extensive calculations are made for the reaction $\pi N \to \pi\pi N$ which account for many features of the observed spectrum, and finally the implications of the model for the reaction $NN \to NN\pi$ are pointed out.

The final conclusion to be drawn from the calculations is that the Drell-Deck diffraction mechanism is multiperipheral in nature, and should always be calculated in such terms.

PART I

a) A Review of High-Energy Scattering Phenomenology

The current experiments in high-energy strong interaction physics consist almost entirely of two-particle scatterings. The experimental techniques available limit these scatterings mostly to cases of π- meson, K - meson, antiproton or proton beams colliding with nucleon targets. But within this apparently limited framework a whole wealth of final states is available. For convenience, the various final states can be assigned to one or other of four classes :

i) Elastic scattering

ii) Charge exchange scattering

iii) Particle production with two final particles

iv) Particle production with more than two final particles .

Strictly speaking, the second class of charge exchange scattering is a subdivision of the third class, the two particle production reactions. Nevertheless charge exchange scattering processes show many unique features which make them worthy of special mention.

For the theorist, the problem is to write down unique matrix elements for all these processes. At the time of writing, this desirable state of affairs has yet to be attained, but the theorist has several powerful weapons at his disposal which to a certain extent on-

enable him to describe with a certain degree of prediction each of the scattering classes referred to above. The weapons number four :

i) Peripheral Particle Exchange

ii) Regge Pole Theory and Complex Angular Momentum

iii) Group Theory

iv) Unitarity

Each particular type of scattering process possesses its own problems which lead one to consider different avenues of approach. Before considering each scattering class in turn, a brief review of the four branches of theory will be made.

For completeness, mention should also be made of the recent developments in high-energy scattering theory which stem chiefly from symmetry properties of the strong interactions. These developments include the Johnson-Treiman relations [1] and the quark model [2]. Each of these has met with a certain amount of success, but they are used chiefly to set up sum rules relating to amplitudes, rather than to specify the form of a single amplitude. For this reason these more modern achievements will not be described here in any detail.

The idea of peripheralism dates back to the notion of virtual photons in electromagnetism and made its first appearance on the stage of nuclear physics with the 'heavy quanta' of Yukawa. The idea is that

the source particles, the nucleons, are surrounded by a cloud of virtual particles, the mesons. The lifetime and range of these mesons are governed by an uncertainty principle, which says that the size of the region of space-time influenced by a virtual particle is inversely proportional to its mass. If it is assumed that the interaction between nucleons is caused by an 'exchange' of virtual mesons, then the long-range interactions will be dominated by a mechanism whereby only the lightest mesons are involved.

In S-matrix language, it is assumed that the u- and t-dependences of the amplitude are dominated by pole terms corresponding to single particle intermediate states in the direct and crossed channel processes. (Here s and t are of course the usual Mandelstam invariants). At high energy one is normally far from any single particle threshold, so the effect of the s-channel poles is not important for these cases. The poles in the crossed channel now give significant contributions as the momentum transfer becomes small. Thus the high energy behaviour in the direct channel is determined essentially by the low-energy behaviour of the physical crossed channel.

One is assuming all the time that the pole contributions to the amplitude dominate over the integrated discontinuities for the various cuts. Pion poles are especially suitable for this purpose since

such a pole at $t=m_N^2$ is very close to small negative values of t compared with the branch point at $t=4m_\pi^2$. For processes which cannot contain pion poles, the single particle pole will often be close to the branch point, and the assumption of pole dominance is not warranted.

Since it is the lightest quanta which are being exchanged, the peripheral premise asserts that the momentum transfers are small, giving rise to final states that are strongly peaked in the forward direction. This is indeed found to be the case for most high-energy scattering, but should not be taken as direct confirmation of the peripheral hypothesis, since it will be shown that several other models produce so-called 'forward peaking'.

Before proceeding, the reader's attention should be drawn to two serious drawbacks to this naive peripheral model. Firstly, no appeal has been made to unitarity. That is to say, although a large part of the scattering amplitude will be due to direct peripheral interactions having large impact parameter, there must be a residual contribution due to 'head-on' collisions which may produce wide-angle elastic scatterings, or may be highly inelastic. The second drawback can best be illustrated by considering a scattering process with two particles in initial and final states. The peripheral model enables the apparent four-point vertex for such an occurrence to be split into two three-point

vertices, these vertices describing the emission and absorption of the exchanged particle. So a knowledge of these vertices is imperative to a meaningful peripheral calculation. The first peripheral calculations [3] surmounted both hurdles by assigning an empirical 'form-factor' to each three-point vertex, the functional form of this factor being deduced by direct comparison with experiment. Although highly unsatisfactory from an aesthetic point of view, this approach nevertheless enabled some degree of prediction to be made.

The different characteristics of elastic and inelastic scatterings would seem to indicate that these processes come about through different workings. Inelastic modes possess a predominantly real amplitude which is accounted for by a simple Born term. Elastic scatterings show a markedly imaginary amplitude which cannot be explained by any simple particle exchange. It is for this purpose that the ideas of Regge poles and complex angular momentum find their chief application. This model provides a way of accounting for the small momentum transfers and large imaginary parts in a manner which still retains links with exchanges of physical particles.

The idea is to write a partial wave expansion for the amplitude in the crossed channel, and then use a Sommerfeld-Watson transform to change the summation over discrete partial waves into a contour integral over a continuous angular momentum variable. Under certain conditions this integration can be dominated by angular momentum poles along the real axis, the Regge poles, and it is assumed that there exists an analytic continuation of this amplitude into the region of the direct channel. If this is so, then the high-energy behaviour in the direct channel is due to the low-lying Regge poles.

The series of Regge poles of similar quantum numbers which occur along the real angular momentum axis is viewed not as a series of objects of differing mass and spin assignments, but as manifestations of a single entity moving in a fixed trajectory across the complex angular momentum plane.

The vacuum exchange mechanism referred to previously is found to be due to two trajectories, the lowest poles of which are identified with the two isosinglet 2^+ mesons with positive G-parity, the f^o (1250) and the f^o (1520). Besides these trajectories, elastic scattering is found to possess finer details which demand for more Regge poles[5]. These are capable of contributing to other types of scattering process and may indeed under certain conditions mask the peripheral particle

exchanges, in just the same way that Regge pole terms dominate over the peripheralism in elastic scattering.

The Regge amplitude can be likened in some ways to the resultant effect of a sum of single particle exchange modes, the different particles being just the Regge recurrences.

The Regge pole model suffers from the same two diseases as does the peripheral model, namely incorrect unitarization and an imprecise knowledge of the internal vertex functions. This is a far greater drawback for the Regge pole case than for the peripheral case since the coupling of a Regge trajectory to physical particles is much harder to calculate than the coupling of, say, three particles together. Thus to a certain extent, today's Regge pole model is in precisely the same stage of development as the peripheral model in the days of Ferrari and Selleri, since all that can be done is for empirical form factors to be introduced to make up for the model's deficiencies. These form factors appear nevertheless quite simple[6], and a great deal of prediction is possible.

The main achievement of group theory in this context is that the form of the three-point vertex functions so necessary for peripheral calculations can now be written down, and in the case of the higher symmetries, can be explicitly compared. For instance a knowledge of SU(3) and charge conjugation is sufficient to enable the invariant couplings

of a vector meson to two pseudoscalar mesons or three vector mesons together to be written[7], but only considerations of higher symmetries such as U(6, 6) or SL(6, C) can provide the relative magnitudes of these couplings[8]. The trouble with these invariant couplings is that they are only approximate, and to obtain realistic results, one has to take into account the 'symmetry breaking', but even the approximate, invariant couplings are more desirable than an empirical form factor. So far, very little work has been done on the Regge vertices using particle symmetries.

The effects of unitarity are far-reaching and often very subtle. Take the case of ordinary elastic scattering. As the incident energy is increased, then more and more inelastic channels open up and, in optical language, the target particle becomes 'blacker'. It is well-known that the diffraction pattern of an opaque object in the path of a beam exhibits an intense maximum in the centre of the geometric shadow, and in the same way high energy elastic scattering displays a very pronounced forward peak. This peak is the working of unitarity rather than any small momentum transfer mechanism. Although unitarity causes most drastic effects in elastic scattering, it has implications in all types of scattering. For two-particle scattering, considerations of unitarity lead directly to the optical theorem, which relates the total cross-section

with the imaginary part of the forward elastic scattering amplitude :

$$\sigma_{TOT}(s) = \frac{1}{4pE_c} \operatorname{Im} T(s, t=0) \quad \cdots \quad 1$$

where p is the magnitude of the initial 3-momentum, and Ec is the energy of each particle in the centre-of-mass frame.

This expression is derived by introducing the discontinuity of the elastic scattering amplitude across the real energy axis. In a similar way a formula can be obtained which defines the imaginary part of any two-particle scattering amplitude, but this will not be reducible to such a simple form as the optical theorem. This immediately shows up a vast deficiency in the simple peripheral model. The simplest peripheral amplitude, the Born term, is wholly real and so necessarily violates unitarity. It is the aim of the absorbtive peripheral model to remedy this deficiency by including an imaginary part to the amplitude deriving from elastic scatterings in the initial and final states[9]. This model lends itself to considerable intuitive appeal and has the further advantage that the absorbtive terms which correct for unitarity can be easily derived from experimental results on elastic scatterings.

For the Regge model, which finds its application chiefly for elastic scatterings, the unitarity corrections involve the sum of all the inelastic channels. Such corrections are much more difficult to picture, and are practically impossible to calculate.

To summarize, it would seem that there exist two main mechanisms for high-energy scattering, the peripheral particle exchange model and the Regge pole model, and that under different circumstances different workings dominate. At present accelerator energies, it appears that elastic scatterings are dominated by Regge modes and at low energies inelastic processes have a tendency to show features of particle exchange, especially when the exchanges involve pions. At higher energies, all processes give indications of Regge behaviour. This would indicate that the Regge model is the more realistic of the two, but unfortunately its precise nature is not as well-known as that of the peripheral model.

The application of the ideas of group theory and absorption serve to put the peripheral model on a very elegant and acceptable basis which can give excellent results[10]. Their explicit use in the Regge theory is severely limited.

b) Elastic Scattering

The differential cross-section for two-particle elastic scattering is related to the effective squared matrix element by the relation

$$\frac{d\sigma}{d\Omega} = \frac{1}{(8\pi)^2 S} |M|^2 \quad . \qquad 2$$

The form of the differential cross-section has a certain correspondence with the normal Airy diffraction pattern consisting of an intense central

maximum surrounded by concentric secondary maxima. In practice it is assumed that the central maximum overwhelms everything else[11] so that a suitable empirical form for the differential cross-section is

$$\frac{d\sigma}{d\Omega} = \frac{d\sigma}{d\Omega}\Big|_0 e^{\lambda t}$$

so that the effective squared matrix element is given by

$$|M|^2 = (8\pi)^2 s \frac{d\sigma}{d\Omega}\Big|_0 e^{\lambda t} \qquad 3$$

where $\frac{d\sigma}{d\Omega}\Big|_0$ is the magnitude of the forward scattering cross-section and t is the squared momentum transfer. The parameter λ describes the sharpness of the forward peak and for all known elastic scatterings is in the range 5 GeV^2 to 10 GeV^2. It should be emphasized that this usual form is only an approximation to the correct Airy function.

$$\frac{d\sigma}{d\Omega} = \frac{d\sigma}{d\Omega}\Big|_0 \left[\frac{2J_1(\theta)}{\theta}\right]^2$$

where θ is the angular substance.

This intense forward peaking produced at high energies is a direct consequence of the impenetrability of the targets to the incident beam, the central maximum being due to diffraction. The impenetrability of the target area is caused by the many inelastic channels open at these high energies. These channels, although producing other final states, cause complete absorption of the incident beam and can be thought of as offering a certain cross-section that is completely impenetrable. As more inelastic channels open up, as happens in general

with increasing beam energy, this effective impenetrable zone increases too. Analogy with physical optics shows that such an increase in cross-section has negligible effect on the resultant diffraction pattern after the area has attained an optimum size, namely an area sufficient to blot out the first few Fresnel zones. This analogy appears to be good since it is found that the diffractive parameter λ has very little energy dependence.

An intermediate step in the derivation of the optical theorem is the statement relating amplitudes :

$$2\,\mathrm{Im}\,T_{aa} = -\sum_n \delta^4(p-p')\,|T_{na}|^2 \qquad 4.$$

where Taa denotes the forward-scattering amplitude. At high energies the summation on the right-hand side involves many inelastic channels and may be considered as a summation over inelastic channels alone. If the entire forward elastic scattering amplitude derives from these inelastic channels, then it will be seen that the forward elastic amplitude is largely imaginary. This does not mean to say that the elastic amplitudes away from the forward direction are completely imaginary, although this is often assumed. These amplitudes can possess a significant real part for two reasons; firstly that the unitarity equation only applies to the forward direction and secondly any direct elastic scatterings, whether inside the central diffraction maximum or not, will give a real term.

Thus a first order empirical approximation for elastic scattering is to assume a purely imaginary matrix element

$$M = 8\pi i \left(s \frac{d\sigma}{d\Omega}\Big|_0\right)^{1/2} e^{\frac{1}{2}\lambda t} \qquad 5$$

which serves satisfactorily for many purposes. But there are many undesirable features, notably the absence of any information on $\frac{d\sigma}{d\Omega}\Big|_0$, the height of the diffraction peak, which must vary with energy. Also, by definition, this form is entirely unsuitable for describing elastic scatterings away from the forward direction. For this latter purpose the Regge pole model is eminently suitable.

The Regge pole formalism for meson-nucleon elastic scattering has been described by many authors[12] and the significant feature is that the amplitude for no spin flip has energy dependence $\sum_i \left(\frac{\cos\theta_{3t}}{2}\right)^{\alpha_i}$ where θ_{3t} is the centre-of-mass scattering angle in the crossed, 't' channel, and α_i are the continuous spin variables, the trajectories. At high energy, this scattering angle is related to the Mandelstam quantity s by

$$s = 2kk'\cos\theta_{3t} \qquad 6$$

where k, k' are the initial and final centre-of-mass momenta. Note that in the physical region for the direct channel, θ_{3t} is necessarily complex and $\cos\theta_{3t}$ tends to become infinite. The spin flip amplitude has energy dependence $\sum_i \left(\frac{\cos\theta_{3t}}{2}\right)^{\alpha_i - 1}$. Since the trajectories are functions of

momentum transfer alone, then this Regge form for the amplitude can be directly tested without prior knowledge of the actual trajectories by examining the s-dependence of the amplitude for fixed momentum transfer, t. If a single trajectory is present, then this s-dependence should exhibit 'shrinking', i. e. the amplitude for a certain fixed momentum transfer should decrease with increasing energy. This behaviour need not necessarily carry through when many trajectories are present.

It would appear that the Regge pole model gives a satisfactory picture of the s-dependence of elastic scattering for fixed t. What of the t-dependence for fixed s ? Experimentally this consists of the intense central diffraction maximum surrounded by residual wide angle scatterings. Although the Regge model gives a central maximum, it is not distinct enough to correspond with the observed one, which is not really surprising since it has been demonstrated how this central maximum owes its existence to the number of intermediate states, whereas the Regge model neglects these effects altogether. In practice, this difficulty is surmounted by assigning to each Regge amplitude a form-factor Ae^{Bt} in the same way as the forward scattering is parametrized by the amplitude shown in equation 5.

Thus the Regge-pole model with form-factor corrections presents the most satisfactory and complete picture of high-energy elastic scattering.

c) Charge-Exchange Scattering

Since charge exchange is a somewhat cumbersome process to talk about in completely general terms it will be expedient to consider here the representative process $\pi^- p \to \pi^0 n$. Both the peripheral exchange[13] and the Regge pole models[14] are capable of prediction, and so this instance provides an instructive borderline case.

The reaction must proceed through three distinct channels. Firstly via the channel containing one intermediate s-channel bound state or resonance, secondly via the exchange of a ρ-meson-like entity carrying one unit of isospin, and thirdly via fermion exchange.

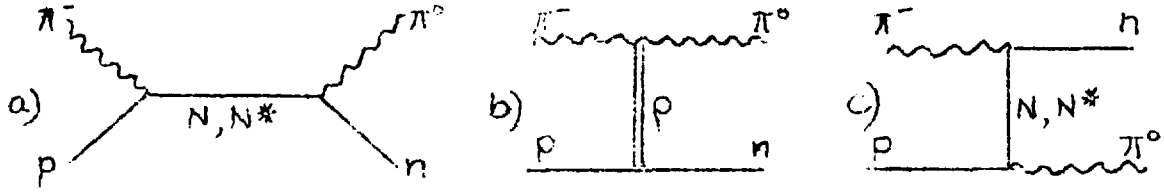

Fig. 1 Mechanisms for charge-exchange scattering

Barger and Cline have shown how N and N^* like entities exist up to masses of 3.2 GeV[15], so the process shown in Fig. 1(a) must be important below, say, 8 GeV incident pion lab. momentum. The high-energy behaviour can be credited to the two exchange processes shown in Figs. 1(b) and 1(c). It is generally assumed that meson exchange in the t-channel is responsible for the forward scattering hemisphere, whereas baryon exchange in the u-channel is responsible for the backward

scattering hemisphere, so that a unique matrix element can be written down.

Although charge exchange is an inelastic process, it constitutes only one of the many inelastic channels open at high energy and so from the point of view of charge exchange scattering, the target particle appears relatively 'black'. This causes the low partial waves to form an intense forward diffraction peak, just as in the case of elastic scattering except that this forward peak is now inelastic. Any Regge pole calculation must then include drastic unitarity factors in order to describe this peaking.

It will be seen that the forward peaking arises as a result of all the possible inelastic channels, so an exact unitarity calculation will be extremely difficult to perform. But it has been shown before how a major part of the forward elastic scattering amplitude owes its existence to precisely this same optical effect. It was the idea of the complete absorption model to take account of the sum of the inelastic channels by introducing initial and final state interactions consisting of forward elastic scattering with no helicity changes. This simplifies the calculation enormously.

Apart from this question of unitarity, the difference between the two theoretical approaches is the specific form of the unit of isospin

exchanged. The absorption model uses an off-mass shell ρ-meson having unique spin one whereas the Regge model uses a ρ-trajectory whose effective mass and effective spin are indeterminate. Although the form of the Regge amplitude is not known as accurately as the particle exchange amplitude, it is of a more general nature and as such could incorporate the features of the particle amplitude. The Regge model introduces into the calculation the effects of the recurrences of the ρ-meson, and the question to be decided is to what extent these recurrences are important compared with the ρ-meson pole. The answer must presumably be energy dependent. It is worthy of note that the absorption calculation for charge exchange scattering mediated by ρ-mesons demands the introduction of further modifications to obtain agreement with experiment, notably the introduction of a complex mass term for the exchanged meson. The Regge model needs no such further modifications although the predictions of this model for polarizations are far from satisfactory and it has been suggested[16] that the introduction of an extra Regge trajectory is required to get the polarizations right.

d) Production Processes with Two Final Particles

For a long while two-particle production processes have been the particular forte of absorption model workers. A great number of

calculations have been made[17] and in several cases striking agreement with experimental data has been achieved. The majority of these instances involve the one-pion-exchange mechanism and the predictions of calculations involving other exchange modes are on the whole less impressive.

The philosophy of peripheralism states that high energy scattering processes are mediated by the exchange of the lightest particles, that the production amplitude is dominated by the particle poles closest to the physical region. This philosophy is certainly very attractive and for a long time there was never any cause to doubt its validity as analysis of actual data always confirmed the presence of single pion exchanges. It was then discovered that certain reactions, which on a peripheral assumption should proceed via pion exchange, displayed the characteristics of a strong vector meson exchange mode[18]. For the reaction $Kp \to K^* p$ at 3 GeV, an analysis of the final decay products of the K* seems to indicate vector meson exchange, which is confirmed by examination of the spin density matrix. Furthermore this vector meson mode becomes more dominant as the energy is increased. This is in complete contradication to the peripheral assumption, which would assert that as the energy is increased and the momentum transfers become correspondingly smaller, the contribution

of the pion pole toward the total amplitude becomes even more significant.

At very high energies, there is then no alternative but to recourse to the Regge pole model and the Regge trajectories themselves, being entirely phenomenological, take the anti-peripheral behaviour into account. But the model, being of such an empirical nature, can offer no explanations for the breakdown of the peripheral assertions.

From the point of view of the Regge model, the dominance of pion exchange for medium energy processes has been a constant source of embarrassment. A general form for one Regge pole amplitude is

$$T = \beta_i(t)\ \frac{1+\exp[-i\pi(\alpha_i-\sigma_i)]}{\sin\pi(\alpha_i-\sigma_i)}\left(\frac{\cos\theta_{3t}}{2}\right)^{\alpha_i} \qquad 7$$

where α_i is the Regge trajectory, σ_i the signature, θ_{3t} the crossed channel centre-of-mass scattering angle and β_i the vertex function which is supposed to contain the Regge pole residue, all renormalizations and a unitarity correction. If this vertex function is of the same order of magnitude for all trajectories, then the dominant trajectory will be that one which contributes most to the angular dependence $\left(\frac{\cos\theta_{3t}}{2}\right)^{\alpha_i}$. It is presumed that for medium energies the pion 'trajectory' although having a small effective spin α_i has an outlandishly large residue β_i, which combined with the effect of its abnormally

low mass, causes it to dominate other unit isospin trajectories. But at high energies this premise is no -longer true and the dominance reverts to the ρ -trajectory.

It would appear that dominance of a pion pole, or any other pole for that matter, must not be presupposed too rashly. On the other hand if the experimental evidence favours a pion pole, then a neat and often very accurate calculation can be carried out.

Finally this is a convenient point to examine the formalism of unitarity for two-particle scattering. This is normally carried out using the usual transition matrix, T, and the real reaction matrix, the K-matrix[19]. The two are linked by an expression

$$T = K - i\pi K \rho T \qquad 8$$

where ρ is a density of states factor. The matrix elements depend both on momentum p, spin s and channel, α, so that a typical 2-particle matrix element has the form $\langle p_i s_i p_j s_j \alpha_{ij} | T | p_m s_m p_n s_n \alpha_{mn} \rangle$. For this reason most authors follow Dalitz[20] and define new quantities

$$T' = (\pi\rho)^{1/2} T (\pi\rho)^{1/2}$$

$$K' = (\pi\rho)^{1/2} K (\pi\rho)^{1/2}$$

which are related by an expression

$$T' = K' - iK'T' \qquad 9$$

which (neglecting spin) has the advantage of involving only channel labels. The expression becomes

$$T'_{\alpha\beta} \simeq K'_{\alpha\beta} - i \sum_{\gamma} K'_{\alpha\gamma} T'_{\gamma\beta} \qquad 10$$

The first term is the usual Born amplitude and the second term including summation over all channels represents the unitarity correction. For elastic scattering the expression reduces to

$$T'_{\alpha\alpha} = K'_{\alpha\alpha} - i \sum_{\gamma} K'_{\alpha\gamma} T'_{\gamma\alpha} \qquad 11$$

This clearly shows the fallacy in assuming a completely imaginary amplitude for elastic scattering. Apart from the Born term, the unitarity correction itself contributes a significant real part to the total amplitude.

It should be emphasized at this juncture that the summation over states theoretically includes those channels which are closed, in the sense that their thresholds have yet to be attained. It is well known that channels just below threshold have serious effects on total amplitudes[21], although channels with distant threshold values can be safely ignored. The series expansion for the T-matrix is :

$$T'_{\alpha\beta} = K'_{\alpha\beta} - (K'_{\alpha\gamma} K'_{\gamma\beta} - K'_{\alpha\gamma} K'_{\gamma\delta} K'_{\delta\beta} + i K'_{\alpha\gamma} K'_{\gamma\delta} K'_{\delta\varepsilon} K'_{\varepsilon\beta} + \cdots$$

where summation over repeated indeces is implied. It is the idea of the absorption model to approximate this by

$$T'_{\alpha\beta} = K'_{\alpha\beta} - i K'_{\alpha\alpha} K'_{\alpha\beta} - i K'_{\alpha\beta} K'_{\beta\beta} - K'_{\alpha\beta} K'_{\beta\delta} K'_{\delta\beta} - K'_{\alpha\gamma} K'_{\gamma\alpha} K'_{\alpha\beta} + \cdots$$

$$= K'_{\alpha\beta} - iK'_{\alpha\beta}(K'_{\beta\beta} - iK'_{\beta\delta}K'_{\delta\beta} - \cdots) - i(K'_{\alpha\alpha} - iK'_{\alpha\delta}K'_{\delta\alpha} - \cdots)K'_{\alpha\beta}$$

$$= K'_{\alpha\beta} - iK'_{\alpha\beta}T'_{\beta\beta} - iT'_{\alpha\alpha}K'_{\alpha\beta}$$

$$= \frac{K'_{\alpha\beta}}{2}(1 - 2iT'_{\beta\beta}) + (1 - 2iT'_{\alpha\alpha})\frac{K'_{\alpha\beta}}{2}$$

$$= \frac{1}{2}\{K'_{\alpha\beta}S_{\beta\beta} + S_{\alpha\alpha}K'_{\alpha\beta}\}$$

In this way the effects of unitarity are allowed for by assuming initial and final state interactions consisting of unitarized elastic scatterings, with no helicity changes. The absorption approximateion involves truncation over only <u>one</u> set of intermediate states, and the elastic correction factors contain the combined effects of many complete sets of intermediate states.

Such an absorption calculation is in principle simple and elegant. The approach fails altogether for the Regge model for two reasons. Firstly that the Regge model is often used to calculate elastic scatterings, and secondly that the real K-amplitude cannot be identified with the complex Regge pole amplitude.

e) <u>Multi-Particle Production Processes</u>

It is with multi-particle production processes at high-energy to which the remainder of this thesis is concerned, and in particular with three-particle final states. Consider the process $a+b \to 1+2+3$

If it is assumed that the interaction is dominated by pole terms, this enables the apparent five-point vertex to be reduced to two smaller verteces in one of the two ways shown in Fig.2. The lines

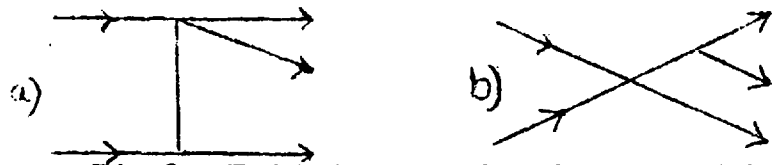

Fig.2 Pole diagrams for single-particle production

have not been explicitly labelled for in some cases each diagram can be meaningfully labelled in several ways. One can proceed in the same way to attack the four-point verteces, to obtain

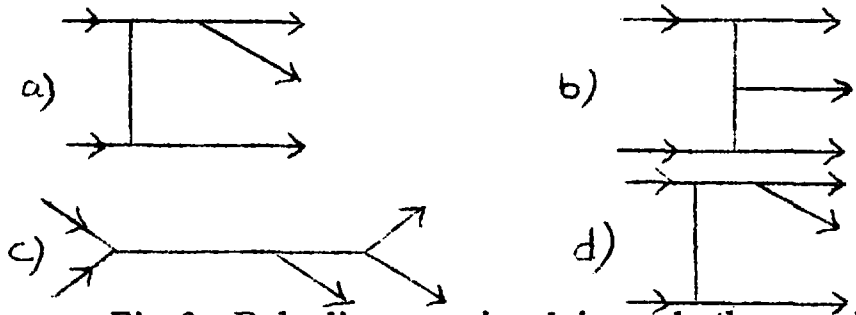

Fig.3 Pole diagrams involving only three-point functions

the set of 'irreducible' diagrams shown in Fig.3. Diagrams 3a and 3b can both be considered as deriving from Diagram 2a, and diagrams 3c and 3d evolve from 2b. Thus although 3a and 3d appear to be the same, they are capable of having different pole terms.

The usual high energy philosophy argues that at high energy one is remote from any s-channel poles, whereas the momentum transfer variable tends to approach zero from below, and the momentum

transfer dependence consequently becomes increasingly dominated by poles in the t-channel. For this reason, diagram 3b is usually spoken of as the 'high-energy diagram', 3a and 3d as medium-energy diagrams and 3c as the low-energy diagram[22]. Before carrying out any calculation, it is important to know precisely the form of the pole dominances, for instance in a Regge picture to include all the relevant trajectories, and for particle exchange to include the correct proportions of pseudoscalar and vector meson exchanges.

If at any time a precise knowledge, however empirical, of a four-point function is obtained, then it is possible to evaluate matrix elements directly for the Fig. 2 diagrams, without having to resort to the irreducible diagrams. This approach will be illustrated in some detail later. It is sometimes possible to perform the reverse process, and starting from the experimental results one can infer a great deal about four-point functions which are otherwise inaccessible. For instance the single pion production process $\gamma p \to \pi\pi p$ is often used to obtain an amplitude for pion-pion scattering[23] which is an extremely difficult experiment to perform using present-day methods.

This reaction class of multi-particle final states also covers the diffraction dissociation processes, the existence of which was first pointed out by Good and Walker[23a]. The idea is that ordinary

diffraction scattering should exhibit in the final state traces of the 'dressing' of the participating particles in the same way as the diffraction pattern of a beam of unpolarized light exhibits a separate pattern for each distinct polarization state. These reactions, which appear distinctly inelastic, might be lumped together with truly elastic diffraction scattering for the purposes of unitarity. This is uncommonly hard to achieve, and for most purposes now diffraction processes are viewed as distinct inelastic modes.

PART 2

a) Notation and Kinematics

This section gives a summary of the notation scheme for the reaction a + b → 1 + 2 + 3 and goes on to define all the angles and kinematical quantities needed in order to calculate differential cross-sections. This is all standard stuff which draws heavily on the work of Wick[24] and Razmi[25].

The two initial particles will be called a and b, and the three final ones 1, 2 and 3. The momenta of the particles will be denoted by a letter p with an appropriate suffix label, and the helicities in a similar way by λ. The process has five linearly independent kinematical invariants. The set to be employed is

$$s_{ab} = (p_a + p_b)^2 \quad , \quad s_{12} = (p_1 + p_2)^2$$
$$s_{23} = (p_2 + p_3)^2 \quad , \quad t_{3a} = (p_3 - p_a)^2 \qquad 16$$
$$t_{1b} = (p_1 - p_b)^2 \ .$$

Thus s always denotes a centre-of-mass energy-squared invariant and t always a squared momentum transfer invariant. From time to time, it will be convenient to use quantities other than those listed above, but which are defined in a similar way. They will be linearly related to the set 16 :

$$s_{12} + s_{23} + s_{31} = s_{ab} + m_1^2 + m_2^2 + m_3^2$$

$$t_{1b} + s_{12} + t_{2b} = t_{3a} + m_1^2 + m_2^2 + m_b^2$$

$$t_{2a} + s_{23} + t_{3a} = t_{1b} + m_2^2 + m_3^2 + m_a^2 \qquad 17$$

$$t_{1b} + t_{2b} + t_{3b} = -s_{ab} + m_1^2 + m_2^2 + m_3^2 \cdots + m_a^2 + 2m_b^2$$

The various energies and three-momenta of the particles can then be expressed in terms of the fundamental set 16. To do this, it is convenient to define a quantity

$$\lambda(a,b,c) = (a^2+b^2+c^2-2ab-2bc-2ca)^{1/2}.$$

In the overall centre-of-mass frame, that in which $\underline{p}_a + \underline{p}_b = 0$, the energies, ω, and three-momentum magnitudes, q, are:

$$q_a = q_b = (2\sqrt{s_{ab}})^{-1}\,\lambda(s_{ab}, m_a^2, m_b^2)$$

$$q_1 = (2\sqrt{s_{ab}})^{-1}\,\lambda(s_{ab}, m_1^2, s_{23})$$

$$q_2 = (2\sqrt{s_{ab}})^{-1}\,\lambda(s_{ab}, m_2^2, s_{31})$$

$$q_3 = (2\sqrt{s_{ab}})^{-1}\,\lambda(s_{ab}, m_3^2, s_{12})$$

$$\omega_a = (2\sqrt{s_{ab}})^{-1}\,(s_{ab} + m_a^2 - m_b^2) \qquad 18$$

$$\omega_b = (2\sqrt{s_{ab}})^{-1}\,(s_{ab} + m_b^2 - m_a^2)$$

$$\omega_1 = (2\sqrt{s_{ab}})^{-1}\,(s_{ab} + m_1^2 - s_{23})$$

$$\omega_2 = (2\sqrt{s_{ab}})^{-1}\,(s_{ab} + m_2^2 - s_{31})$$

$$\omega_3 = (2\sqrt{s_{ab}})^{-1}\,(s_{ab} + m_3^2 - s_{12})$$

To specify the angular dependences to be outlined shortly, the energies and momenta measured in the frame where $\underline{p}_1 + \underline{p}_2 = 0$, the Q-frame, must be known. These are :

$$
\begin{aligned}
q_a^Q &= (2\sqrt{s_{12}})^{-1}\lambda(s_{12}, m_a^2, t_{3b}) \\
q_b^Q &= (2\sqrt{s_{12}})^{-1}\lambda(s_{12}, m_b^2, t_{3a}) \\
q_1^Q &= q_2^Q = \tfrac{1}{2}\left[s_{12} - (m_1+m_2)^2\right]^{1/2} \\
q_3^Q &= (2\sqrt{s_{12}})^{-1}\lambda(s_{ab}, m_3^2, s_{12}) \\
\omega_a^Q &= (2\sqrt{s_{12}})^{-1}(s_{12} + m_a^2 - t_{3b}) \\
\omega_b^Q &= (2\sqrt{s_{12}})^{-1}(s_{12} + m_b^2 - t_{3a}) \\
\omega_3^Q &= (2\sqrt{s_{12}})^{-1}(s_{ab} + m_3^2 - s_{12}) \\
\omega_2^Q &= (2\sqrt{s_{12}})^{-1}(s_{12} + m_2^2 - m_1^2) \\
\omega_1^Q &= (2\sqrt{s_{12}})^{-1}(s_{12} + m_1^2 - m_2^2)
\end{aligned}
\qquad 19
$$

There are three angles which must be known in order to compute cross-sections, and a fourth angle which will be needed later. This last quantity is the polar scattering angle Θ_3 in the centre-of-mass of the three-particle final state and is given by

$$
\cos\Theta_3 = \frac{1}{2q_a q_3}\left(t_{3a} - m_a^2 - m_3^2 + 2\omega_a\omega_3\right) \qquad 20
$$

The other three angles are θ_3 and φ_3, which are the scattering angles for particle 3 in the Q-frame, and χ_2. χ_2 can be considered as the mutual scattering angle of particles 1 and 3 in the overall centre-of-mass frame. They are defined by

$$\cos\theta_3 = \frac{1}{2q_2^Q q_3^Q}\left(-s_{23} + m_2^2 + m_3^2 + 2\omega_2^Q\omega_3^Q\right) \qquad 21$$

$$\cos\chi_2 = \frac{1}{2q_3 q_1}\left(s_{12} + s_{23} - s_{ab} - m_2^2 + 2\omega_3\omega_1\right) \qquad 22$$

$$\sin\chi_2\cos\varphi_3\sin\Theta_3 + \cos\chi_2\cos\Theta_3 = \frac{1}{2q_1 q_b}\left(-t_{1b} + m_b^2 + m_1^2 - 2\omega_1\omega_b\right) \qquad 23$$

The differential cross-section for the reaction

a + b → 1 + 2 + 3 is

$$d^5\sigma = \frac{1}{(2\pi)^5 F}\sum|T|^2\,\delta^4(P_f - P_i)\,\frac{d^3q_1\,d^3q_2\,d^3q_3}{2\omega_1\,2\omega_2\,2\omega_3} \qquad 24$$

where F denotes the incident flux, $4\sqrt{s_{ab}}\,q_a$, and $\sum|T|^2$ represents the squared matrix element for the process summed over final spin states and averaged over initial spin states.

Transforming to angular variables and integrating trivially over Φ, the overall orientation,

$$d^4\sigma = \frac{1}{32(2\pi)^4}\cdot\frac{q_1^Q q_3}{q_a\sqrt{s_{12}}\sqrt{s_{ab}}}\sum|T|^2\,d(\cos\theta_3)\,d\varphi_{13}\,d\omega_3\,d(\cos\Theta_3) \qquad 25$$

$$ds_{23}\,dt_{1b}\,ds_{12}\,dt_{3a} = 16\sqrt{s_{ab}}\,q_1^Q q_3^Q q_a^2 q_1 q_3\sin\chi_2\sin\varphi_{13}\sin\Theta_3\,d(\cos\theta_3)\times\cdots \qquad 26$$
$$\cdots\times d\varphi_3\,d\omega_3\,d(\cos\Theta_3)$$

so that the final expression for the cross-section becomes

$$d^4\sigma = \frac{1}{512(2\pi)^4} \cdot \frac{\sum |T|^2}{S_{ab}\sqrt{S_{12}}\, q_{ba}^3 q_1 q_3^2 \sin\chi_2 \sin\varphi_3 \sin\theta_3}\, ds_{23}\, ds_{12}\, dt_{1b}\, dt_{3a} \qquad 27$$

It is this formula which will be used to calculate the differential cross-sections $d\sigma/ds$, these being the effective squared-mass spectra for two-particle subsystems in the three-particle final states.

b) Possible Kinematical Enhancements in Three-Particle Final States

It is in the mass-spectra of many-particle final states that the various resonances of the elementary particles are seen. These spectra are very rich in detail and the study of their fine-structure is often a controversial matter with experimentalists. In order to study these finer details more carefully it is usually necessary to subtract out those parts of the spectrum which are dominant overall, for instance the ρ-meson will dominate the mass-spectrum of a two-pion final state and must be removed by a selection of the kinematics for the various events comprising the spectrum. As more resonances are identified and then removed successively, the remaining spectrum approaches that of the 'background' process, that is the process in which the particles seen in the final state are formed directly, without any

s-channel resonance being produced which would subsequently decay.

In view of the number of lesser enhancements seen in the different two-particle subsystems of a three-particle final state, it was suggested that some of these effects might be produced merely by the kinematics of the processes concerned[26], rather than by a genuine production mechanism. That is to say that these enhancements could be merely groupings round a particular effective mass value brought about by kinematical effects which could superficially show up like particle resonances.

The idea was first applied to the $\rho\pi$ sub-system in the reaction $\pi p \to \rho\pi p$[27]. The existence of the A_2 (1324) resonance was generally accepted but it was hoped that the lower enhancement at 1080 MeV, called by some the A_1 meson[28], could be explained away on this new basis. The mechanism is shown by the two diagrams in Fig. 4. The dark blobs denote elastic diffraction scatterings on the proton, which participates in the process merely as a 'spectator' particle, one which reacts only kinematically and takes no dynamical role at all. In both instances shown it should be expected

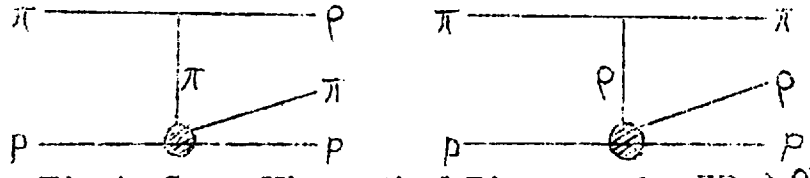

Fig. 4 Some Kinematical Diagrams for $\pi p \to \rho\pi p$

that the $\rho\pi$ effective mass will show an enhancement at the lower end of the spectrum.

If the incident pion lab. energy is T, then the corresponding centre-of-mass incident energy is

$$W = \sqrt{s_{ab}} = +\sqrt{\left[(m_\pi + m_p)^2 + 2 T m_p\right]} \qquad 28$$

The minimum effective mass is simply $m_\pi + m_\rho$, and the maximum is $W - m_p$.

The problem now is to determine whether the effects of these processes can be responsible for pseudo-resonance behaviour. It was the claim of the earliest calculations[27] that this in fact was the case. These calculations were however very crude, involving many approximations in the kinematics, which is perhaps undesirable in the calculation of an effect which is supposed to be kinematical in origin. And in addition to this fairly superficial objection it might be argued that if these diagrams, which are perhaps the simplest which can be attributed to this specific production process, themselves give rise to mass-spectrum enhancements, to what diagram or diagrams belongs the remaining 'background' spectrum. That is unless the background spectrum itself contains an intrinsic enhancement from which it cannot be disassociated.

Furthermore it could be presumed that this behaviour could be now exhibited in all production processes a + b → 1 + 2 + 3 which contain a 'spectator' particle, which can participate in the reaction merely as a target for elastic diffraction scattering. To this end the next section presents a comprehensive survey of the effects of diffraction scattering in the reaction type a + b → 1 + 2 + 3.

c) The Role of Diffraction Scattering in Production Processes

This section shall deal exclusively with the reaction a + b → 1 + 2 + 3 which contains one spectator particle. There are three important examples of this type, namely

$$\pi p \rightarrow \rho \pi p$$
$$Kp \rightarrow K^{*} \pi p$$
$$\pi p \rightarrow \pi \pi p$$

These reactions will be considered in turn in some detail, and there are further examples, e.g. $\pi p \rightarrow \omega \pi p$, which will not be touched upon here, but are governed by the same general principles.

The effect of diffraction scattering in these processes is due to the three diagrams shown in Fig. 5, together with their interference terms. Again the blobs show where

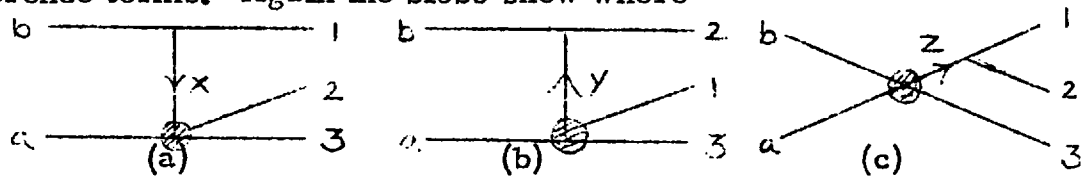

Fig. 5 Diffraction Scattering in Production Processes

the diffraction scattering takes place and the quantities x, y, z represent the four-momenta of the propagated particles. To correspond to the reaction $\pi p \to \rho \pi p$, the identification needed is

$$a \equiv p, \quad b \equiv \pi, \quad 1 \equiv \rho, \quad 2 \equiv \pi, \quad 3 \equiv p$$

For $Kp \to K^* \pi p$, the corresponding identification is

$a \equiv p, b \equiv K, 1 \equiv K^*, 2 \equiv \pi, 3 \equiv p$ and finally for

$\pi p \to \pi \pi p, a \equiv \pi, b \equiv p, 1 \equiv p, 2 \equiv \pi, 3 \equiv \pi$

In these diagrams the diffraction vertex will be described by an imaginary function whose squared modulus is that of equation 3.

This was the form of the matrix element for 2-particle on-shell diffraction, and it is being tacitly assumed that the 4-point vertex function describing off-shell scattering is of precisely the same form.

The matrix element for each diagram will be constructed from three factors, the imaginary four-point elastic scattering vertex function, a real propagator term and an inelastic three-point vertex function. This vertex will be the same for each diagram, and so the matrix elements for each diagram will have the same phase, giving a maximum possible total effect.

Since each matrix element contains an empirical four-point vertex function, it is not possible to construct the matrix element and

perform spin summations in strict accordance with the Feynman rules. All that can be done is for a squared matrix element, summed and averaged over the appropriate spin states, to be written in a semi-phenomenological way, in a form dictated by the Feynman techniques. These squared matrix elements are respectively for the three diagrams:

$$\sum |T_a|^2 = \sum |E^a_{b12}|^2 \frac{1}{(x^2 - m_2^2)^2} |M_{23}|^2$$

$$\sum |T_b|^2 = \sum |E^b_{b12}|^2 \frac{1}{(y^2 - m_1^2)^2} |M_{13}|^2 \qquad 29$$

$$\sum |T_c|^2 = \sum |E^c_{b12}|^2 \frac{1}{(z^2 - m_b^2)^2} |M_{ob}|^2$$

The summation signs denote a summation over final spin states and an average over initial ones. E_{b12} is the common inelastic three-point vertex function and the M's are the various elastic form factors. Thus the total effective squared matrix element for the process is

$$\sum |T|^2 = \sum |T_a|^2 + \sum |T_b|^2 + \sum |T_c|^2 + \cdots$$

$$\cdots + 2\sqrt{\left[\sum |T_a|^2 \sum |T_b|^2\right]} + 2\sqrt{\left[\sum |T_a|^2 \sum |T_c|^2\right]} + \cdots \qquad 30$$

$$\cdots + 2\sqrt{\left[\sum |T_b|^2 \sum |T_c|^2\right]} .$$

d). Some Explicit Examples

Consider first the reaction $Kp \to K^* \pi p$. As mentioned before, the diagrams for this process are obtained from the general ones in Fig. 5 by the identification

$$a \equiv p,\ b \equiv K,\ 1 \equiv K^*,\ 2 \equiv \pi,\ 3 \equiv p$$

For the first diagram, in which the kaon goes into a K* and an off-shell pion, the three-point vertex is

$$\sum |E^a_{b12}|^2 = \frac{1}{4} g^2_{K^*K\pi} (p_b + x)_\mu (p_b + x)_\nu \left[-g_{\mu\nu} + \frac{p_{1\mu} p_{2\nu}}{m^2_{K^*}} \right] \qquad 31$$

The squared coupling constant $g^2_{K^*K\pi}$ will contain a Clebsch-Gordan coefficient characterizing the precise charge mode being calculated. This vertex function reduces to

$$\sum |E^a_{b12}|^2 = \frac{g^2_{K^*K\pi}}{4 m^2_{K^*}} \left[x^2 - (m_K + m_{K^*})^2 \right] \left[x^2 - (m_K - m_{K^*})^2 \right] \qquad 32$$

In the second diagram, the kaon goes into a pion and an off-shell K* :

$$\sum |E^b_{b12}|^2 = \frac{1}{4} g^2_{K^*K\pi} (p_2 + p_b)_\mu (p_2 + p_b)_\nu \left[-g_{\mu\nu} + \frac{y_\mu y_\nu}{y^2} \right] \qquad 33$$

$$= \frac{g^2_{K^*K\pi}}{4 y^2} \left[y^2 - (m_K + m_\pi)^2 \right] \left[y^2 - (m_K - m_\pi)^2 \right] \qquad 34$$

Finally for the third diagram,

$$\sum |E^{c}_{b12}|^2 = \frac{1}{4} g^2_{K^*K\pi} (z+p_2)_\mu (z+p_2)_\nu \left[-g_{\mu\nu} + \frac{p_{1\mu} p_{2\nu}}{m^2_{K^*}} \right] \qquad 35$$

$$= \frac{g^2_{K^*K\pi}}{4 m^2_{K^*}} \left[z^2 - (m_{K^*} + m_\pi)^2 \right] \left[z^2 - (m_{K^*} - m_\pi)^2 \right] \qquad 36$$

Many experiments have been carried out for both πp and Kp elastic scattering at various energies, and the necessary parameters $d\sigma/d\Omega|_0$ and λ are well established, so there is no difficulty in writing the elastic form factors for these diagrams. Data for $K^* p$ elastic scattering is almost impossible to obtain, so in the absence of such data the only thing left to do is to assume these parameters to be the same as those for the Kp case. But as would be expected from a pole calculation, the diagram with the pion pole dominates completely over the diagram with the K* - meson pole with the result that the second diagram can be neglected in the actual calculation. Whether this in fact is realistic is another matter completely, since at very high energies the Regge recurrences of the K* pole may cause significant effects.

The effective squared matrix elements for the two important diagrams are then -

$$\sum |T_a|^2 = \frac{g^2_{K^*K\pi}}{4m^2_{K^*}} \left[x^2 - (m_K + m_{K^*})^2\right]\left[x^2 - (m_K - m_{K^*})^2\right] X \cdots$$

$$\cdots X \frac{1}{(x^2 - m_\pi^2)^2}(8\pi)^2 S_{23} \left.\frac{d\sigma}{d\Omega}\right|_{0,\pi p} e^{\lambda_{\pi p} t_{3a}}$$

$$\sum |T_c|^2 = \frac{g^2_{K^*K\pi}}{4m^2_{K^*}} \left[z^2 - (m_{K^*} + m_\pi)^2\right]\left[z^2 - (m_{K^*} - m_\pi)^2\right] X \cdots$$

$$\cdots X \frac{1}{(z^2 - m_K^2)^2}(8\pi)^2 S_{ab} \left.\frac{d\sigma}{d\Omega}\right|_{0,Kp} e^{\lambda_{Kp} t_{3a}} \qquad 37$$

The elastic parameters, especially $d\sigma/d\Omega|_0$, are strictly speaking energy dependent, but the variation over S_{23} will be ignored and S_{ab} is of course held fixed for each particular experiment.

Fig. 6 shows the results of a calculation for an incident K-particle laboratory momentum of 6 GeV. The histogram shows the experimental results for the effective squared mass of the K* π sub-system of the final state and is due to a collaboration between the Birmingham, Glasgow, Imperial College London, Munich, Oxford and and Rutherford Laboratory experimental groups[29]. The solid curve shows the prediction of the two (really three) diagrams assuming maximum interference. The dashed curve shows the contribution due to the first diagram containing one-pion-exchange. The discussion of these

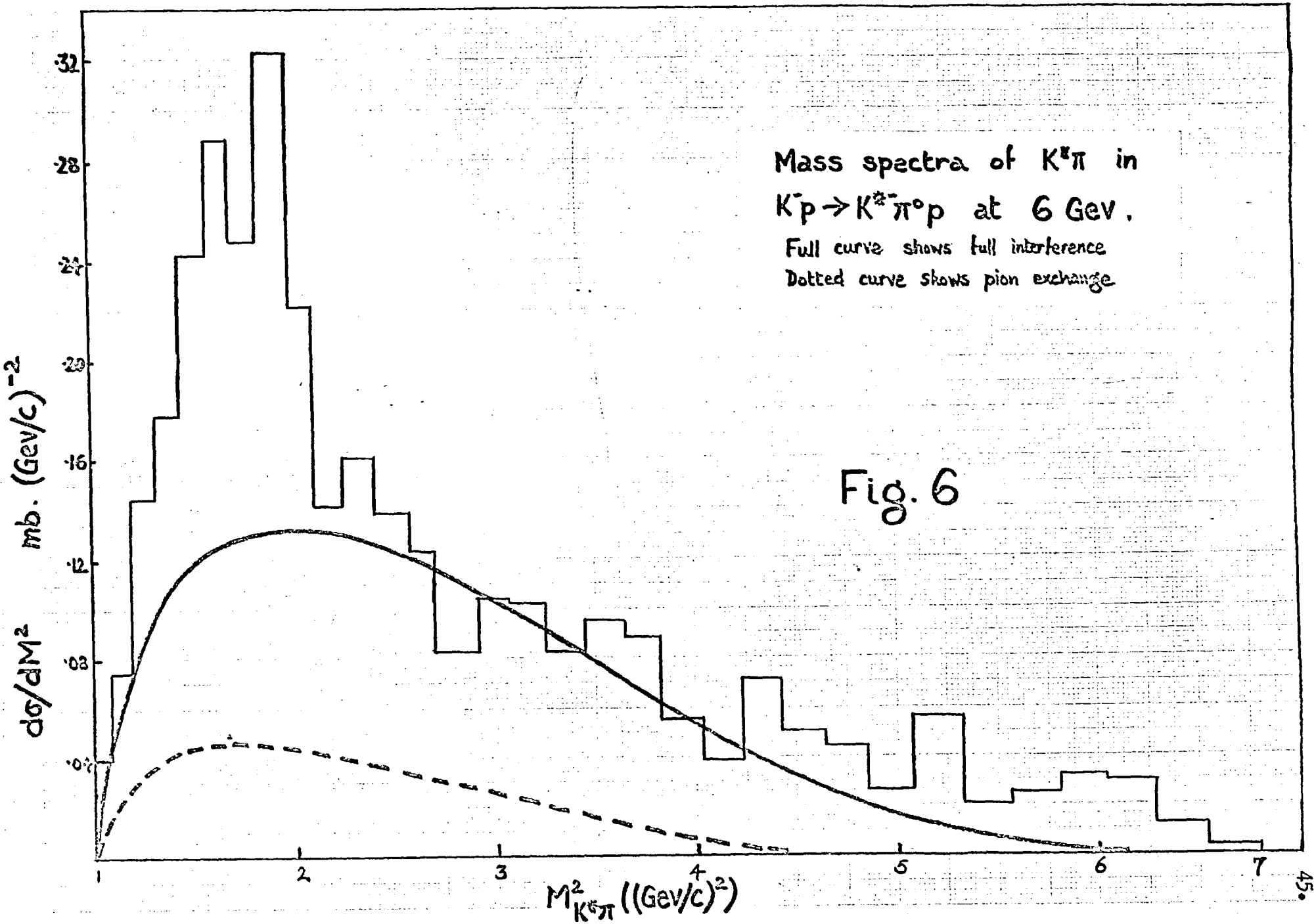
Mass spectra of $K^{\pm}\pi$ in
$K^-p \to K^{*-}\pi^0 p$ at 6 Gev.
Full curve shows full interference
Dotted curve shows pion exchange
Fig. 6
$d\sigma/dM^2$ mb. $(Gev/c)^{-2}$
$M^2_{K^{\pm}\pi}$ $((Gev/c)^2)$
45°

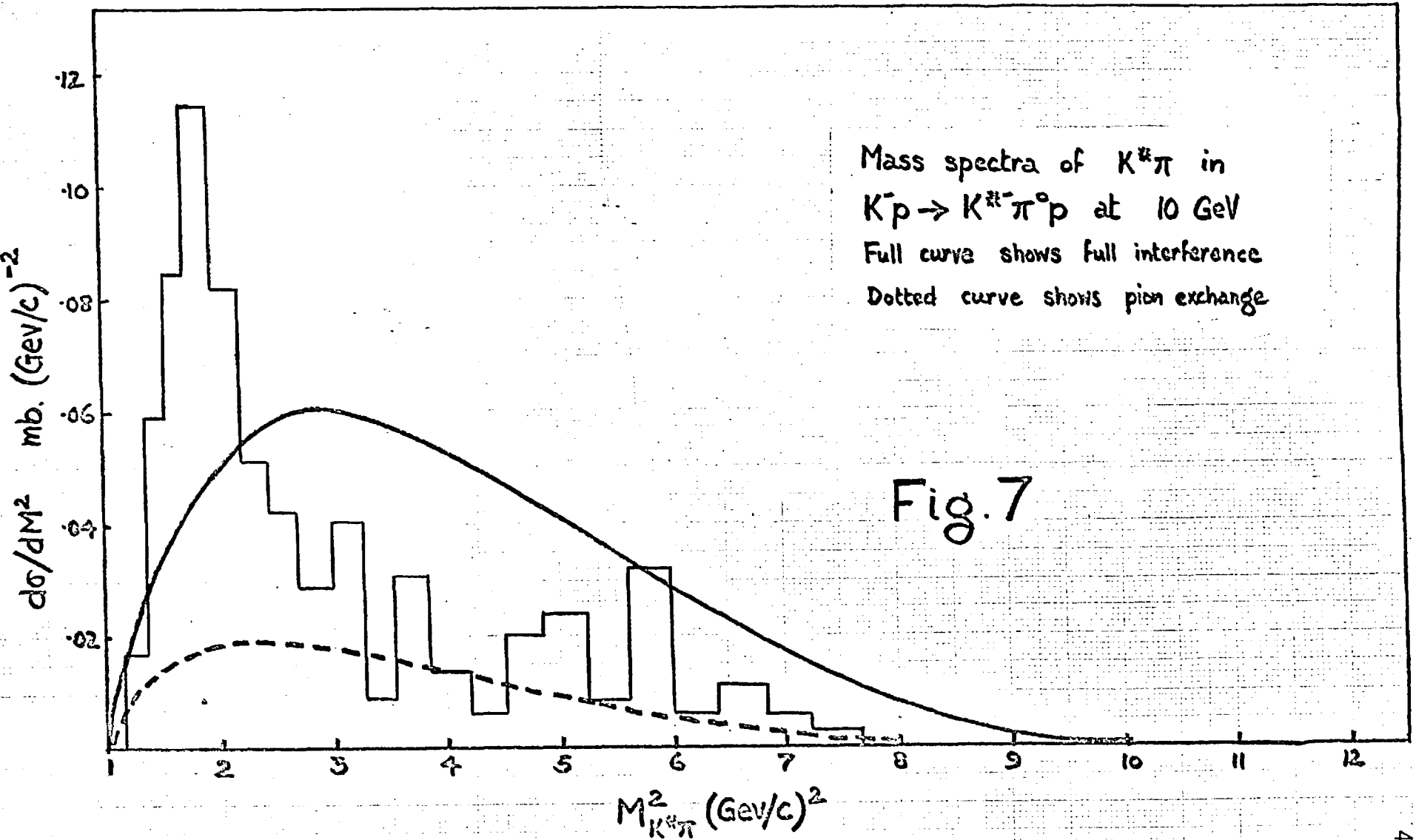
Mass spectra of $K^{*}\pi$ in
$K^{-}p \rightarrow K^{*-}\pi^{0}p$ at 10 GeV
Full curve shows full interference
Dotted curve shows pion exchange
Fig. 7
$d\sigma/dM^2$ mb. $(GeV/c)^{-2}$
$M^2_{K^{*}\pi}$ $(GeV/c)^2$
·12
·10
·08
·06
·04
·02
1
2
3
4
5
6
7
8
9
10
11
12

results and their implications is postponed until the next section. Fig. 7 shows the corresponding results for 10 GeV K-particle laboratory momentum. Here the experimental histogram is due to the Aachen, Berlin, CERN, Imperial College London, Vienna collaboration[30].

The next reaction to be considered is that of $\bar{\pi}p \to p\bar{\pi}p$

$$a \equiv p\,,\quad b \equiv \bar{\pi}\,,\quad 1 \equiv \rho\,,\quad 2 \equiv \bar{\pi}\,,\quad 3 \equiv p$$

The analysis of this reaction is very similar to the previous one since in both cases the inelastic three-point vertex involves a vector meson and two pseudoscalar mesons.

$$\sum |T_a|^2 = \frac{g_{\rho\pi\pi}^2}{4m_\rho^2}\left[X^2-(m_{\bar{\pi}}+m_\rho)^2\right]\left[X^2-(m_\pi-m_\rho)\right]^2 X \cdots$$

$$\cdots X \frac{1}{(X^2-m_{\bar{\pi}}^2)^2}(8\bar{\pi})^2 S_{23}\left.\frac{d\sigma}{d\Omega}\right|_{0,\bar{\pi}p} e^{\lambda_{\bar{\pi}p} t_{3a}} \quad \text{and}$$

$$\sum |T_c|^2 = \frac{g_{\rho\pi\pi}^2}{4m_\rho^2}\left[Z^2-(m_\rho+m_{\bar{\pi}})^2\right]\left[Z^2-(m_\rho-m_\pi)^2\right] X \cdots$$

$$\cdots X \frac{1}{(Z^2-m_{\bar{\pi}}^2)^2}(8\bar{\pi})^2 S_{ab}\left.\frac{d\sigma}{d\Omega}\right|_{0,\bar{\pi}p} e^{\lambda_{\bar{\pi}p} t_{3a}} \qquad 38$$

Fig. 8 shows the resulting $\rho\pi$ mass distribution for 8 GeV pion lab. momentum compared with the experimental statistics[31]. Again the solid curve corresponds to maximum interference between diagrams and the dotted curve is the contribution of one-pion-exchange alone.

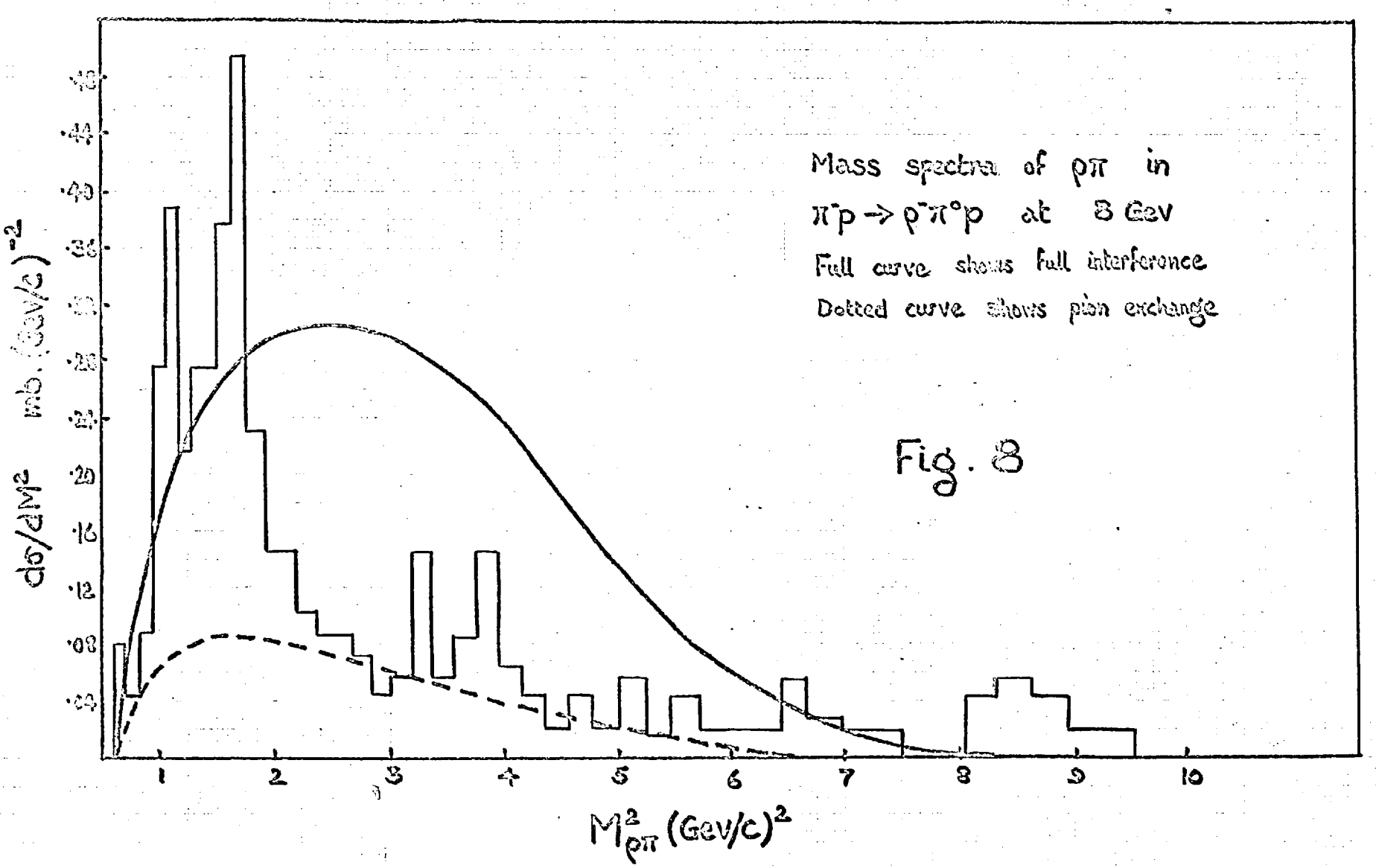
Mass spectra of pπ in
π⁻p → p⁻π⁰p at 8 Gev
Full curve shows full interference
Dotted curve shows pion exchange
dσ/dM² mb. (Gev/c)⁻²
M²pπ (Gev/c)²
1
2
3
4
5
6
7
8
9
10

Fig. 8

The final calculation is for $\bar{\pi}p \to \bar{\pi}\bar{\pi}p$ at 8 GeV pion laboratory momentum.[32]

$$a \equiv \bar{\pi},\quad b \equiv p,\quad 1 \equiv p,\quad 2 \equiv \bar{\pi},\quad 3 \equiv \pi$$

Again for a pole calculation the contribution of the second diagram containing nucleon exchange can be neglected in comparison with a one-pion-exchange diagram. The effective squared matrix elements turn out to be

$$\sum |T_a|^2 = \frac{g^2_{NN\pi}}{(x^2 - m^2_{\pi})^2} (8\pi)^2 s_{23} \frac{d\sigma}{d\Omega}\Big|_{0,\bar{\pi}\pi} e^{\lambda_{\bar{\pi}\pi} t_{3a}}$$

and

$$\sum |T_c|^2 = \frac{g^2_{NN\pi}}{(x^2 - m^2_{N})^2} (8\pi)^2 s_{ab} \frac{d\sigma}{d\Omega}\Big|_{0,\bar{\pi}p} e^{\lambda_{\bar{\pi}p} t_{3a}} \qquad 39$$

There are several points about this calculation. Firstly it might appear strange that one diagram containing a nucleon pole is insignificant whereas another (the third) contributes significantly. This is because the nucleon poles are in the t- and s-channel modes, respectively, and at medium energies the s-channel pole still has a sizeable effect on the overall matrix element.

Secondly there occurs a difficulty with the parametrizations for pion-pion scattering. Such an experiment is almost impossible to perform using present-day techniques, with the result that no numerical values are at hand for the two elastic scattering

parameters. But for all the elastic scattering data available so far, the exponential parameter λ is always in the range 6 - 10 GeV, and it would seem reasonable to suppose that the corresponding parameter for pion-pion scattering is also of this magnitude. The actual numerical value assigned is of no great consequence, the amplitude not being very sensitive to this exponential factor anyway. The other parameter, namely the scale parameter $d\sigma/d\Omega|_o$ is an entirely different proposition. For the moment this quantity will be left as a free parameter which will be determined by the requirement that the contribution of the first diagram shall be of the same order of magnitude, but nevertheless greater than, the contribution of the third diagram. Obviously this is not an accurate procedure, but is nevertheless sufficient to determine the relative orders of magnitude of the pion-pion and pion-nucleon forward elastic scattering cross-sections.

Actual calculation shows that in order to get a sensible comparison between the two major contributing diagrams for this process, the pion-pion forward elastic scattering differential cross-section $d\sigma/d\Omega|_o$ must be depressed by a factor of ten compared with the experimentally determined quantity from pion-nucleon scattering. This is an interesting result which will be touched upon again in Part 3. Fig. 9 shows the results of the calculation for the

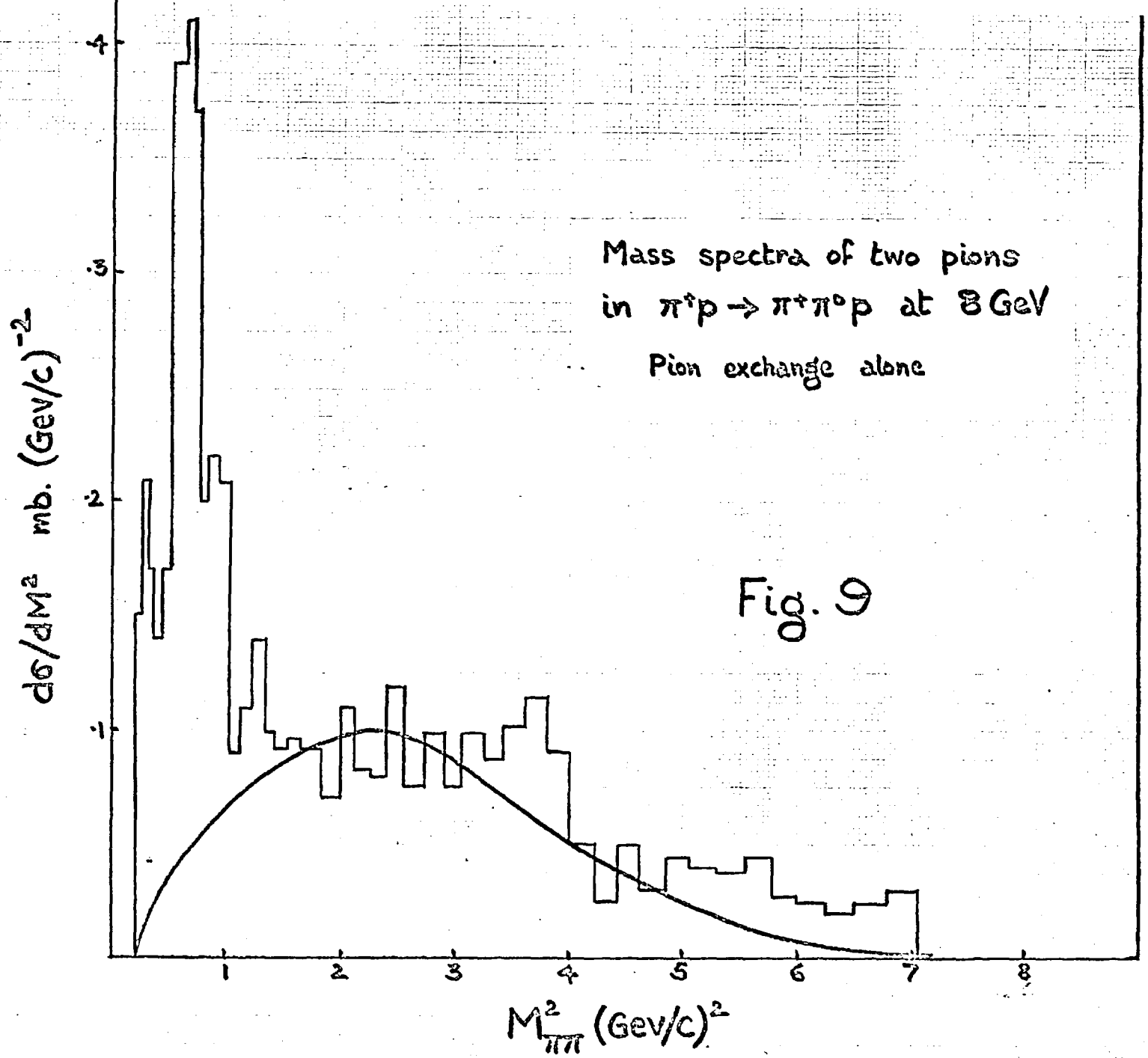
Mass spectra of two pions
in $\pi^+p \to \pi^+\pi^0 p$ at 8 GeV
Pion exchange alone
$d\sigma/dM^2$ mb. $(Gev/c)^{-2}$
$M^2_{\pi\pi}$ $(Gev/c)^2$
1
2
3
4
5
6
7
8
·1
·2
·3
·4

Fig. 9

mass spectrum of the two pions in the reaction $\pi p \to \pi\pi p$, for 8 GeV pion laboratory energy.

e). Discussion

Consider again the general process shown in Fig. 5(a). Both the momentum transfer variables t_{1b} and t_{3a} are necessarily small, with the result that particle 2 is of relatively low energy in the overall centre-of-mass frame. For this reason both the 12 and 23 subsystems will display a larger differential cross-section in the low-mass region. On the other hand the 13 subsystem will tend to have fairly high energy, so the mass-distribution should peak up towards the phase space limit. For Fig. 5(c), these peakings will still exist but will be less apparent, with the result that a combination of the two diagrams will shift any enhancement towards the centre of the mass distribution.

The results of the one-pion exchange diagram calculations shown in Figs. 6, 7, 8, 9 display clearly the enhancement of the cross-section in the low mass region, in a manner which could not be predicted by any statistical phase-space model. But these accumulations are not distinct enough to be mistaken for resonances. Genuine resonances have a width less than a few hundred MeV whereas the widths of these calculated mass distributions extend over several GeV.

The effects of maximal interference between possible contributing diagrams also show low-mass enhancements, but again these are much too broad ever to be mistaken for resonances. It has been assumed that the diagrams contribute exactly in phase, since each diagram has a purely imaginary contribution. This assumption could prove wrong, and violent phase changes between diagrams could conceivably give rise to a pseudo-resonance effect. Such violent changes seem unlikely though, and all the evidence so far seems to indicate that a reasonably smooth mass-distribution will be obtained in each case.

If the cross-sections corresponding to resonance production are deducted from the total cross-section for the particular process one obtains a quantity which represents the cross-section for direct particle production. This quantity will be frequently referred to from now on, and will be termed the 'background' cross-section. The corresponding processes in which the final three particles are produced without any intermediate s-channel resonances or isobars occurring will be termed 'background processes'. If the experimentally observed enhancements are subtracted from the overall cross-section, then the resulting mass distribution resembles very closely in shape those calculated. It appears that virtual diffraction of an exchanged pion provides a quite satisfactory fit to the background

spectrum, especially at higher energies.

There are several other points which should be mentioned at this stage. The one diagram 5(c) containing the s-channel pole should be carefully examined before attributing its effect to the background spectrum, since although the pole is not itself of a resonant nature, it could be associated in some way with poles which are of a resonant nature. This is particularly true with nucleon poles and will be discussed again in Part 3. In these cases where 5(c) is not a valid diagram for the background spectrum, then 5(a) alone is the mechanism responsible for direct particle production.

Another point is the fact that the amplitudes for resonance production and the background process interfere with each other, with the result that the apparent widths of the resonances as seen from the mass distributions are not the 'true' widths of the resonances. This should be borne in mind when making simple Breit-Wigner fits to resonance production[33].

These calculations serve to indicate the general nature of kinematical effects in single particle production, how they produce a smooth mass-distribution free of pseudo-resonance effects. At the same time this background mass spectrum is considerably different

from that which would be predicted by a statistical phase-space model. The final part of the thesis sets out to examine the details of this residual spectrum by more sophisticated means.

PART 3

a) Introduction

The investigations in Part 2 indicated the existence of a definite background spectrum for direct single particle production, but the techniques employed were not sophisticated enough to predict the form of the background spectrum in detail. Hitherto the elastic scattering has been presumed to possess a purely imaginary vertex function, i.e. the elastic scattering mechanism has been assumed to proceed entirely through the diffraction process. This assumption is not correct. It has been shown[34] that even on-shell elastic scattering possesses a significant real part which arises from direct scatterings. The imaginary part is due mainly to the effects of unitarity, but a direct elastic scattering could also conceivably possess an additional imaginary portion.

The idea of this section is to write vertex functions for the elastic scattering in terms of the Regge pole formalism, and it is hoped that such a formulation will be able to produce a more complete picture of the background spectrum. It is this Regge pole picture which is normally used to describe the experimental results for two-particle elastic scatterings, rather than a simple diffraction picture.

The formalism for pion-nucleon scattering has been studied extensively[12] and the differential cross-section is usually written in the rather asymmetrical form

$$\frac{d\sigma}{dt} = \frac{1}{\pi s}\left(\frac{m_N}{4k}\right)^2\left\{\left(1-\frac{t}{4m_N^2}\right)|F_{++}|^2+\frac{t}{4m_N^2}\left(s-\frac{s+p^2}{1-t/4m_N^2}\right)|F_{+-}|^2\right\} \quad 40$$

Here p is the pion laboratory momentum, k is the centre-of-mass momentum, F_{++} is the non-flip amplitude and F_{+-} is the helicity flip amplitude.

These helicity amplitudes are assumed to be dominated by a number of Regge poles. For pion-nucleon scattering at least three such poles are needed to fit the experimental data. One of these poles is the Pomeranchuk pole, P, which governs the asymptotic limit of the high-energy scattering, whilst the other two, namely a second vacuum pole P' and the ρ pole of isospin one, are needed to provide the systematic variation of the amplitudes from the asymptotic limit and to account for the variation with charge mode. The contributions of each pole towards the different helicity amplitudes are normally written

$$F_{++i} = C_i\left[\frac{1+e^{-i\pi(\alpha_i-\sigma_i)}}{\sin\pi(\alpha_i-\sigma_i)}\right](\cos\theta_{3t})^{\alpha_i} \quad 41$$

$$F_{+-i} = D_i\left[\frac{1+e^{-i\pi(\alpha_i-\sigma_i)}}{\sin\pi(\alpha_i-\sigma_i)}\right](\cos\theta_{3t})^{\alpha_i-1} \quad 42$$

where α_i and σ_i are the trajectories and signatures of the various Regge poles. C_i and D_i are vertex functions which contain the residues of the poles and must also be amended for the effects of unitarity. The quantity θ_{3t} is the centre-of-mass scattering angle in the crossed channel, which becomes in general complex in the physical region for the direct scattering process.

To obtain these expressions for the amplitudes, it is necessary to assume that the Legendre polynomials $P(\alpha, \cos\theta_{3t})$ arising from the angular momentum analysis in the crossed channel behave like $(\cos\theta_{3t})^{\alpha}$. This assumption is justified only when $\cos\theta_{3t} \to \infty$

The general expression for $\cos\theta_{3t}$ is[35]

$$\cos\theta_{3t} = \frac{(t+m_1^2-m_2^2)(t+m_3^2-m_4^2) + 2t(s-m_1^2-m_3^2)}{\sqrt{\left[\{t-(m_1+m_2)^2\}\{t-(m_1-m_2)^2\}\{t-(m_3+m_4)^2\}\{t-(m_3-m_4)^2\}\right]}} \qquad 43$$

where the s-channel corresponds to $1 + \bar{3} \to \bar{2} + 4$, and the t-channel to $1 + 2 \to 3 + 4$. It is easy to show that $\cos\theta_{3t}$ tends to become infinite for large s and small t only if $m_1 = m_2$, $m_3 = m_4$. That is, the normal Regge asymptotic form holds good only for elastic scattering. For all other cases this asymptotic form is suspect.

The vertex functions C_i and D_i should be regarded at

this stage as pure phenomenological form factors. Very little theoretical work has been done as yet on the residues of Regge poles, or on the unitarity corrections to Regge amplitudes, and certainly nothing is known about their combined effect. They are usually parametrized as

$$C_i = C_{i0}\,\alpha_i(t)\{2\alpha_i(t)+1\}\exp(C_{i1}t) \qquad 44$$

$$D_i = D_{i0}\,\alpha_i(t)\exp(D_{i1}t) \qquad 45$$

Where $\alpha_i = 0$, the scalar nature of the exchange process rules out the possibility of spin-flip. This is the reason for the presence of the α_i factor in the D_i vertex function. Empirically it is found that a number of Regge trajectories pass through $\alpha = 0$ in the region of negative t, and unless something is done about it, these poles will contribute towards the amplitude in the normal way. It is generally assumed that the actual Regge poles must correspond to real physical particles, and for this reason those Regge poles which occur in the negative t region are undesirable. They are usually termed 'nonsense' or 'ghost' states and are removed by placing suitable zeros in the numerators of the expressions for the amplitudes.

Ghost states will occur in general whenever trajectories with even signature pass through even integers for negative t and when those with odd signature pass through odd integers. In practice, the only ghost states which are troublesome are those arising when $\alpha = 0$. The factors α_i serve just this purpose in the vertex functions for the non-flip amplitudes; they cancel the zero occurring in the denominator when α_i becomes zero which would otherwise give rise to a pole term. Finally the exponential factors provide the intense forward peaking brought about by unitarity.

b) Formalism

This section will deal with the general formulation of scattering amplitudes for single particle production involving particles of arbitrary spin. The mechanism adopted will be that of the twin-exchange multiperipheral diagram shown in Fig. 10. Each of the exchanges will be assumed to arise from the resultant contribution of an arbitrary number of Regge poles.

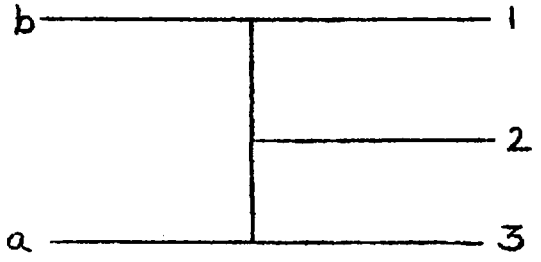

Fig. 10 Twin-exchange diagram for single particle production

The objection might be raised that this diagram alone is not sufficient to account for the complete high-energy background spectrum, and that the diagrams involving s-channel poles should be included, (see Fig. 3), as was done in the investigations into diffraction scattering. This is a valid point, but it is hoped that by excluding those events in the experimental results which definitely correspond to resonance production, the effect of these s-channel poles will be minimized. There can still remain s-channel poles, notably the nucleon pole, which do not correspond to resonance production but have a large coupling strength. The nucleon pole is in reality the first manifestation of a moving Regge pole which is responsible for a whole series of nucleon-type resonances[15], so vestigial effects of this diagram remain even after resonance production events are selected out. Happily it turns out that the experimental data has a background spectrum which is dominated by the twin-exchange multiperipheral diagram. The residual contribution due to s-channel poles can be readily identified and is of minor importance. The mode of calculation is now sufficiently sophisticated for the contributions of the candidate diagrams to the background spectrum to exhibit markedly different behaviour. This was not possible with the diffraction calculations.

The procedure for constructing the amplitude follows

closely that due to Kibble[22] and Razmi[25]. The Regge poles correspond to physical particle poles in an annihilation process, so what is done in all Regge analyses is to first construct the amplitude for a 'crossed' process which contains the correct annihilation mode, and then change variables to obtain the corresponding amplitude for the 'direct' or s-channel scattering process. Thus for example, pion-nucleon scattering at high-energy is assumed to be dominated by t-channel poles which are just those which occur in the s-channel for nucleon-antinucleon annihilation into two pions. So really the diagram which will be under consideration, at least initially, is that shown in Fig. 11, in which all poles occur in the direct channel. When dealing with this crossed diagram, all quantities will be primed, to avoid confusion. Any unprimed quantity refers explicitly to the high-energy diagram in Fig. 10. The connexion between the particle

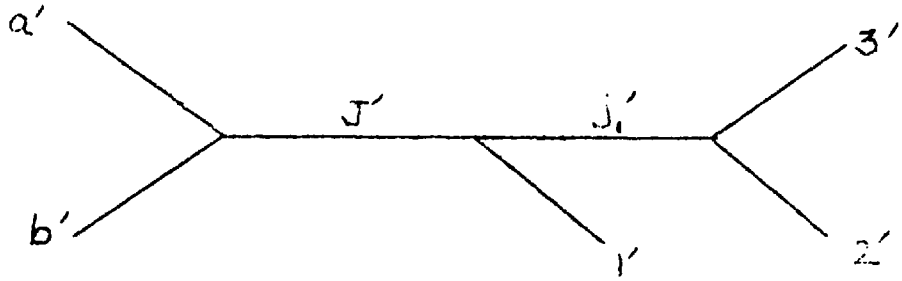

Fig. 11 Low-energy Diagram for Angular Momentum Analysis

labellings is :

$$a' \equiv a\,,\quad b' \equiv \bar{3}\,,\quad 1' \equiv 2\,,\quad 2' \equiv 1\,,\quad 3' \equiv \bar{b}\,,$$

where a bar denotes the relevant antiparticle. All the kinematical expressions listed at the start of Part 2 will still apply here, provided primed quantities are used consistently throughout.

Before embarking on the angular momentum analysis in the in the usual Wick manner, it will be necessary to at least indicate the meanings of the various angles which arise. The angles are shown schematically in

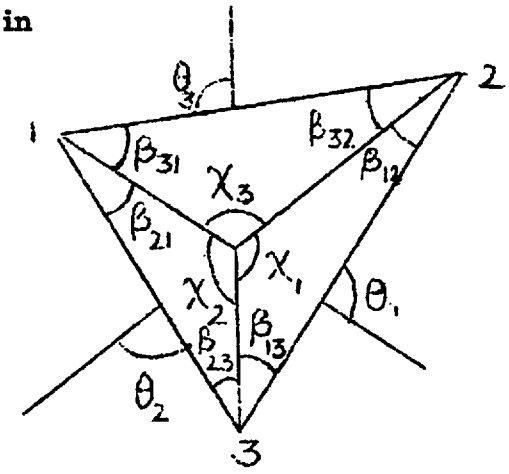

Fig. 12 The Wick Triangle

Fig. 12, the famous Wick Triangle. The various angles β_{ij} are Wigner rotations induced by boosting particle j to the 2-particle centre-of-mass system i.

There are three distinct ways of performing the angular momentum analysis corresponding to the couplings $(12)3$, $(23)1$ and $(31)2$ of the final state particles. For the coupling $(23)1$,

$$T^{\lambda_a'\lambda_b'}_{\lambda_1'\lambda_2'\lambda_3'} = \sum_{\substack{J',j_1',m_1' \\ \nu_3'\nu_2'}} e^{-i\pi S_2'} d^{S_3'}_{\lambda_3'\nu_3'}(\beta_{32}') d^{S_2'}_{\lambda_2'\nu_2'}(\beta_{23}') \times \cdots$$

$$\times d^{j_1'}_{m_1',\nu_3'-\nu_2'}(\theta_3') \mathcal{D}^{J'}_{\lambda_a'-\lambda_b',m_1'-\lambda_1'}(\Phi_3', \Theta_3', \Phi_3') \times \cdots$$

$$\times \langle S_{ab}'J', S_{32}'j_1'm_1'\nu_3'\nu_2'\lambda_1' | T | S_{ab}'J', \lambda_a'\lambda_b' \rangle$$

46

where λ' denotes helicity and ν_3' helicity, S' denotes spin and m' its component, j_1' is the angular momentum of the $(2'3')$-subsystem and J' is the total angular momentum.

$$T^{\lambda_a'\lambda_b'}_{\lambda_1'\lambda_2'\lambda_3'} = \sum_{\substack{J',j_1',m_1' \\ \nu_3',\nu_2'}} e^{-i\pi S_2} d^{S_3'}_{\lambda_3'\nu_3'}(\beta_{32}') d^{S_2'}_{\lambda_2'\nu_2'}(\beta_{23}') \times$$

$$\times d^{j_1'}_{m_1',\nu_3'-\nu_2'}(\theta_3') e^{i(m_1'-\lambda_1')\Phi_3'} d^{J'}_{\lambda_a'-\lambda_b',m_3'-\lambda_3'}(\Theta_3') \times$$

47

$$\times e^{i(\lambda_a'-\lambda_b')\Phi_3'} \langle S_{ab}'J', S_{32}'j_1'm_1'\nu_3'\nu_2'\lambda_1' | T | S_{ab}'J', \lambda_a'\lambda_b' \rangle$$

There is a simplification which can be made at this stage which will eliminate the Wigner rotations β. Eventually the squared modulus of the transition amplitude must be summed over spins. The summation over λ_3' and λ_2' involves a quantity

$$\sum_{\lambda_3'} d^{s_3'}_{\lambda_3'\nu_3'}(\beta_{32}') d^{s_3'}_{\lambda_3'\nu_3''}(\beta_{32}') \sum_{\lambda_2'} d^{s_2'}_{\lambda_2'\nu_2'}(\beta_{23}') d^{s_2'}_{\lambda_2'\nu_2''}(\beta_{23}')$$
$$= \delta_{\nu_3'\nu_3''}\,\delta_{\nu_2'\nu_2''}$$

Bearing in mind that this summation will be done at some time, the angular decomposition can be rewritten in a much simpler form.

$$T^{\lambda_a'\lambda_b'}_{\lambda_1'\lambda_2'\lambda_3'} = \sum_{\substack{J',j_1',m_1' \\ \nu_1',\nu_2'}} e^{-i\pi s_2} e^{i(m_1'-\lambda_1')\varphi_3'} d^{j_1'}_{m_1',\nu_3'-\nu_2'}(\theta_3') \chi$$
$$\chi e^{i(\lambda_a'-\lambda_b')\Phi_3'} d^{J'}_{\lambda_a'-\lambda_b',m_3'-\lambda_3'}(\Theta_3') \langle s',J',j_1',\nu'\lambda_1'|T|\lambda_{a,b}'\rangle \quad 48$$

At this point the Regge trajectories will be introduced. They will be denoted by $J_i' = \alpha_{1i}(s_{ab}')$ and $j_{1i}' = \alpha_{2i}(s_{23}')$, and their respective signatures by σ_{1i} and σ_{2i}. Using these quantities define new amplitudes :

$$\langle s_{ab}'J',s_{23}'j_1'm_1'\nu_1'\nu_2'\lambda_1'|T^{\sigma_{1i}\sigma_{2j}}|s_{ab}'J'\lambda_a'\lambda_b'\rangle =$$

$$\frac{1}{4}\left[1+(-1)^{J_i'-\sigma_{1i}}\right]\left[1+(-1)^{j_{1j}'-\sigma_{2j}}\right]\left[N(J',\lambda_a'-\lambda_b')\times\cdots\right.$$

$$\left.\times N(J',m_1'-\lambda_1')\,N(j_1',m_1')\,N(j_1',\nu_3'-\nu_2')\right]^{-1}\times\cdots$$

$$\times\langle S_{ab}'J',S_{23}'j_1'm_1'\nu_1'\nu_2'\lambda_1'|T|S_{ab}'J',\lambda_a'\lambda_b'\rangle \qquad 49$$

where $N(j,\lambda)=\left[(j+\lambda)!(j-\lambda)!\right]^{1/2}$

Introduce some new d - functions defined like

$$d_{mm'}(j,\cos\theta)=N(j,m)\,N(j,m')\,d^{j}_{mm'}(\theta)$$

and employ these new functions to write the angular momentum decomposition in contour integral form.

$$T^{\lambda_a'\lambda_b'}_{\lambda_1'\lambda_2'\lambda_3'}=\sum'_{m_1',\nu_3',\nu_2'}\sum'_{i,j}e^{-i\pi S_2}e^{i(m_1'-\lambda_1')\phi_3'}e^{i(\lambda_a'-\lambda_b')\Phi_3'}\times\cdots$$

$$\times\int_{C_1}\int_{C_2}dJ'dj_1'\;\frac{d_{m_1',\nu_3'-\nu_2'}(j_1',\cos\theta_3')}{\sin\pi(j_{1j}'-\sigma_{2j})}\cdot\frac{d_{\lambda_a'-\lambda_b',m_1'-\lambda_1'}(J',\cos\Theta_3')}{\sin\pi(J'-\sigma_{1i})}\times\cdots$$

$$\times\langle S_{ab}'J',S_{23}'j_1'm_1'\nu_3'\nu_2'\lambda_1'|T^{\sigma_{1i}\sigma_{2j}}|S_{ab}'J',\lambda_a'\lambda_b'\rangle \qquad 50$$

The contours C_1 and C_2 enclose the region where the integrands are

analytic. Perform the integration and assume that the contributions from the poles along the real axes, the Regge poles, dominate over the remaining 'background integral', in the usual way.

$$T^{\lambda_a'\lambda_b'}_{\lambda_1'\lambda_2'\lambda_3'} = \sum_{m_1',\nu_3',\nu_2'} \sum_{i,j} e^{-i\pi s_2} e^{i(m_1'-\lambda_1')\varphi_3'} e^{i(\lambda_a'-\lambda_b')\Phi_3'} \times \dots$$

$$\times \frac{\pi}{2\sin\pi(\alpha_{1i}'-\sigma_{1i})} \left[d_{\lambda_a'-\lambda_b', m_1'-\lambda_1'}(J_i', \cos\Theta_3') + (-1)^{\sigma_{1i}-\lambda_a'+\lambda_b'} \times \dots \right.$$

$$\left. \times d_{\lambda_a'-\lambda_b', -m_1'+\lambda_1'}(J_i', -\cos\Theta_3') \right] \frac{\pi}{2\sin\pi(\alpha_{2j}'-\sigma_{2j})} \left[d_{m_1',\nu_3'-\nu_2'}(J_{1j}', \cos\theta_3') \right.$$

$$\left. + (-1)^{\sigma_{2j}-m_1'} d_{m_1',-\nu_3'+\nu_2'}(J_{1j}', -\cos\theta_3') \right] \beta_{ij}(s_{ab}', s_{23}', \lambda') \,. \qquad 51$$

Here β_{ij} contains the effective residues of the amplitudes $T^{\sigma_{1i}\sigma_{2j}}$ at the various Regge poles J_i', J_{3j}'. Finally an asymptotic form for the d'- functions will be employed[22), 36)].

$$d_{\lambda,\mu}(\alpha, z) = (-i)^{\lambda-\mu} \Gamma(2\alpha+1) \left(\frac{z}{2}\right)^{\alpha} \qquad 52$$

This will give a final asymptotic form for the crossed channel amplitudes. Several results have been anticipated in the derivation,

notably the discarding of the Wigner rotation terms. Also the asymptotic form used is not valid for the physical region of the crossed channel amplitude, but only for the region where the cosines of scattering angles become large, which corresponds to the physical region for the direct channel.

The problem now is to extract the amplitude for the direct process. For a two-particle scattering process this would involve a Fierz-type transformation scheme and a generalization of this approach to particle production processes would quickly become unwieldy. One idea is to use the two-particle crossing relations established by Trueman and Wick[37] by compounding suitable particle states until the production process takes the form of a quasi-two-particle scattering[38].

c) Single Pion Production

After this hefty chunk of abstruse formalism, this might be a convenient point to consider an explicit process which provides a great simplification to the mathematics but which is still of great practical importance. It is the process of single pion production in pion-nucleon collisions, $\pi N \to \pi\pi N$. The crossed channel process which is then relevant for the angular momentum analysis is nucleon-anti-nucleon annihilation into three pions, $N\bar{N} \to 3\pi$. The

identification with the general process shown in Fig. 10 is

$a \equiv N,\ b \equiv \pi,\ 1 \equiv \pi,\ 2 \equiv \pi,\ 3 \equiv N$.

G-parity forces the assignment of G-parity plus to one propagator and G-parity minus to the other. In the crossed process, the Regge trajectories contributing towards the total angular momentum J' turn out to be the G-minus ones, and the G-plus ones belong to the angular momentum J_1' . The candidate G-minus entities are the pion, and the three trajectories R, ω and φ whilst those for positive G are the usual trio of Pomeranchuk, P , second Pomeranchuk P' and ρ . Nucleon exchange processes are ruled out on the grounds that they are relatively unlikely, and such mechanisms would be immediately recognizable by producing backward rather than forward production of the final state particles involved.

The angular momentum J' will be assumed to be dominated by a pion pole to the exclusion of the trajectories R, ω and φ . Although such an assumption is suspect in the crossed channel, there can be no doubt about the dominance of single pion exchange in a large class of scattering processes in the medium energy range. It turns out eventually that the positive G-parity contributions are dominated completely by the two Pomeranchuk trajectories, P and P' , the

ρ contribution being negligible. Since the R, ω and φ trajectories enjoy a comparable position in the Regge hierarchy to the ρ, there is every reason to presume that their contribution too will be small.

To return to the angular momentum analysis. For the crossed channel $N\bar{N} \to 3\pi$, the expression 51 reduces to

$$T' = \sum_{m_i'} \sum_{i,j} e^{im_i'\varphi_3'} e^{i(\lambda_a' - \lambda_b')\Phi_3'} \frac{\pi}{2\sin\pi(\alpha_{ii}' - \sigma_{ii})} X \cdots$$

$$X \left[d_{\lambda_a' - \lambda_b', m_i'}(J_i', \cos\Theta_3') + (-1)^{\sigma_{ii} - \lambda_a' + \lambda_b'} d_{\lambda_a' - \lambda_b', -m_i'}(J_i', -\cos\Theta_3') \right] X \cdots$$

$$X \frac{\pi}{2\sin\pi(\alpha_{2j}' - \sigma_{2j})} \left[d_{m_i', 0}(j_{ij}', \cos\theta_3') + (-1)^{\sigma_{2j} - m_i'} X \cdots \right.$$

$$\left. X\, d_{m_i', 0}(j_{ij}', -\cos\theta_3') \right] \beta_{ij}(s_{ab}', s_{23}', \lambda') \qquad 53$$

Writing in the pion strictly in Feynman form so that $\alpha_{ii} = 0$ gives

$$T' = \sum_j e^{i(\lambda_a' - \lambda_b')\Phi_3'} \frac{1}{s_{ab}' - m_\pi^2} \cdot \frac{\pi}{2\sin\pi(\alpha_{2j}' - \sigma_{2j})} X \cdots$$

$$X \left[d_{0,0}(j_{ij}', \cos\theta_3') + (-1)^{\sigma_{2j}} (j_{ij}', -\cos\theta_3') \right] \beta_{ij}(s_{ab}', s_{23}')$$

54

Finally use the asymptotic form 52 to obtain

$$T' = \frac{1}{s'_{ab} - m_\pi^2} \sum_j \frac{\pi \beta_{ij}(s'_{ab}, s'_{23})}{2 \sin \pi(\alpha'_{2j} - \sigma_{2j})} \left[1 + e^{-i\pi(\alpha'_{2j} - \sigma_{2j})} \right] \left(\frac{\cos \theta'_3}{2} \right)^{\alpha'_{2j}} \qquad 55$$

It has been anticipated here how a summation over spin states for unpolarized nucleons will eliminate the spin orientation factor $e^{i(\lambda'_a - \lambda_b)\Phi'_3}$. It is generally assumed that the residue term is factorizable into its component vertex parts, the so-called 'factorization hypothesis'. This would mean that β_{ij} can be written

$$\beta_{ij}(s'_{ab}, s'_{23}) = \beta_i(s'_{ab}) \beta_j(s'_{23})$$

where β_i describes the coupling of the nucleon-antinucleon pair to the pion, and β_j is now a form-factor for the pion-pion scattering within the diagram. β_i will be taken to be the normal pion-nucleon coupling constant, $g_{NN\pi}$, so that the amplitude looks like

$$T' = \frac{g_{NN\pi}}{s'_{ab} - m_\pi^2} \sum_j \frac{\pi \beta_j(s'_{23})}{2 \sin \pi(\alpha'_{2j} - \sigma_{2j})} \left[1 + e^{-i\pi(\alpha'_{2j} - \sigma_{2j})} \right] \left(\frac{\cos \theta'_3}{2} \right)^{\alpha'_{2j}} \qquad 56$$

This is now effectively a single amplitude free from helicity labels, and it is a simple matter to write the amplitude for the direct channel.

All that has to be done is to rewrite the amplitude in terms of the invariants for the s-channel mode. The explicit connexion between this set and the dashed set used for the crossed channel is :

$$s'_{ab} \equiv t_{3a}, s'_{12} \equiv s_{12}, s'_{23} \equiv t_{1b}, t'_{3a} \equiv s_{ab}, t'_{1b} \equiv s_{23},$$

so that the actual form for the amplitude for the production process whichis computed is

$$T = \frac{g_{NN\pi}}{t_{3a} - m_\pi^2} \sum_j \frac{\pi \beta_j(t_{1b})}{2 \sin \pi(\alpha_j - \sigma_j)} \left[1 + e^{-i\pi(\alpha_j - \sigma_j)}\right] \left(\frac{\cos \theta'_3}{2}\right)^{\alpha_j} \quad (57)$$

This shows clearly how the amplitude essentially splits into two portions; one part for the pion-nucleon coupling and a second purely Regge-type term which refers to the internal pion-pion scattering.

The factors β_j are parametrized in the form shown in equation 44, but must be regarded as purely empirical at this stage. The exponential parameters C_{1j} show very little variation for investigations of two-particle scatterings[5] and it might be hoped that similar parameters will be valid for this instance of pion-pion scattering. A similar assumption about the parametrization of analysis of single pion production described in Part 2. So the three parameters C_{0j} remain. These determine the absolute scale of

the contributions to the total amplitude from the various Regge poles, and will be frequently referred to as 'scale parameters'. These scale parameters have been fixed for the verteces of P, P' and ρ trajectories in pion-nucleon scattering[5] and are of comparable magnitude. If this holds true for the case under consideration, then the final contribution of the ρ pole is totally negligible. It seems highly unlikely that $C_{0\rho}$ would be inordinately large just for this one case. So now just two parameters remain, namely C_{0P} and $C_{0P'}$. The ratio of these numbers gives the relative coupling strengths of the Pomeranchuk and second Pomeranchuk poles for this particular reaction. It would be very convenient to assume that this ratio takes the same value here as for the case of pion-nucleon scattering, to leave just one free parameter which determines essentially the absolute magnitude of the cross-sections. Using these arguments it is possible to ascertain the structure of the mass-distributions without any free parameters occurring in the calculation. The assumption that the ratio $C_{0P}/C_{0P'}$ is fixed from pion-nucleon analysis is perhaps objectionable, but the calculations turn out to be pretty insensitive to this ratio anyway, the kinematics being the dominant factor.

Fig. 13 shows the predicted form for the two-pion mass

distribution for $\pi^+p \to \pi^+\pi^0p$ at 8 GeV compared with the experimental statistics[32]. These statistics have been selected as those which correspond to the background process of direct pion production, all events corresponding to the resonance production in the final state having been removed. This selection is ready effected by considering the experimental Dalitz plot shown in Fig. 14. The regions 1, 2, 3 correspond to resonance

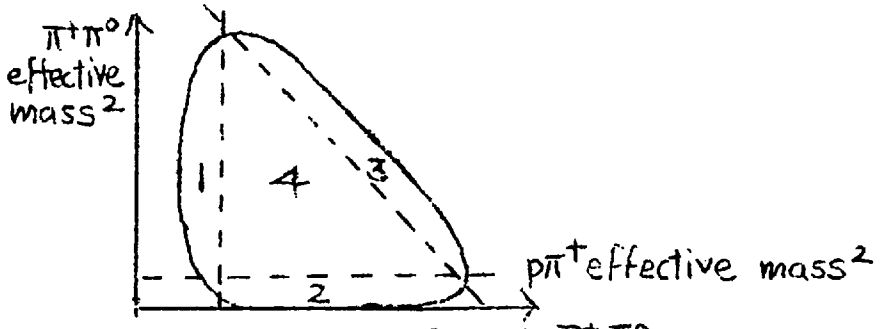

Fig. 14 Dalitz plot for $\pi^+p \to \pi^+\pi^0p$

production in the $p\pi^+$, $\pi^+\pi^0$ and $p\pi^0$ two-particle subsystems respectively. The remaining region 4 in the centre of the Dalitz plot contains those events of genuine pion production, and the histogram in Fig. 13 shows how these events are not isotropically distributed over the available phase space. Thus any explanation of the background spectrum in terms of a statistical model is doomed. The calculated mass-spectrum does exhibit a marked asymmetry, being confined to the lower half of the theoretically available phase space and is effectively zero above 5 GeV^2. Such behaviour can

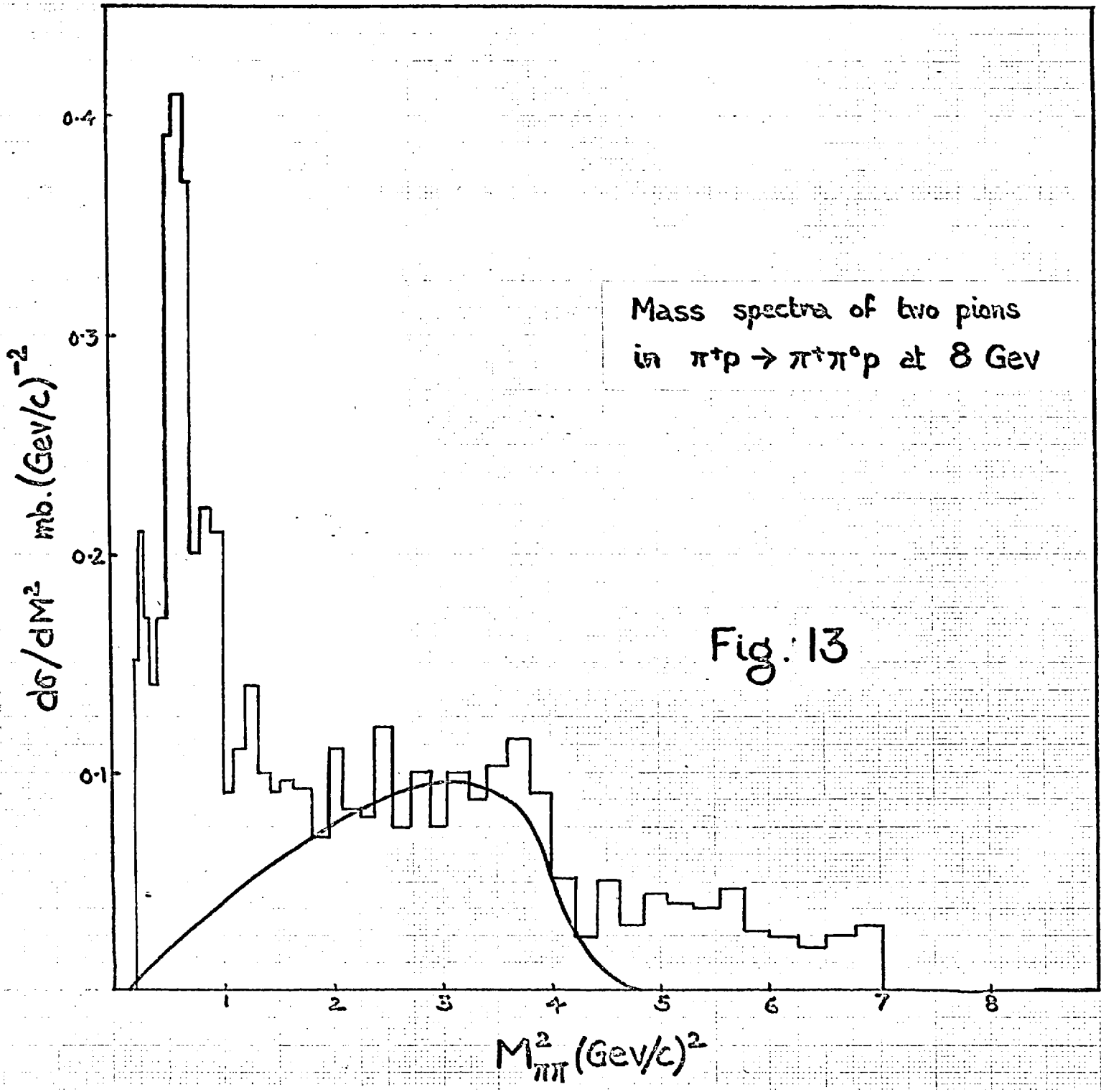
Mass spectra of two pions
in $\pi^+p \to \pi^+\pi^0 p$ at 8 Gev
Fig. 13
$d\sigma/dM^2$ mb. (Gev/c)$^{-2}$
0·4
0·3
0·2
0·1
1
2
3
4
5
6
7
8
$M^2_{\pi\pi}$ (Gev/c)^2

account for some 70% of the observed total cross-section, but it is significant that the maxima of the calculated and the observed mass-spectra coincide exactly near 3 GeV^2. This suggests that this picture of the background mechanism is pretty accurate, the remaining 30% of the total cross-section being due to the vestigial effects of the s-channel resonance diagrams alluded to previously. Since these diagrams contribute mainly to resonance production, it would be an extremely difficult job to try to calculate this remaining portion of the background.

Imagine the incident pion and the target nucleon with its associated pion cloud sweeping toward each other in the overall centre-of-mass frame. The idea of the model is that the incident pions undergo elastic scatterings with the virtual pions, which subsequently materialize as physical pions. The nucleons thus take a minor role in the scattering process, and can be considered merely as 'spectator' particles, so that many of the features of the final state are characteristic of pion-pion scattering. The position of the observed maximum in the two-pion mass spectrum corresponds to the centre-of-mass energy of 8 GeV pions incident on stationary pions in the laboratory, and the structure of the spectrum about this maximum value derives from the explicit momentum transfer dependence in the mechanism. Any population of the upper portion of the

available two-pion spectrum would correspond to large momentum transfers away from the nucleon, the phase-space limit occurring when the final-state nucleons are actually stationary in the overall centre-of-mass frame.

On purely qualitative arguments, the model requires the final state π^+- mesons to have a tendency to be produced strongly in the forward direction, the nucleons in the backward direction and the π^0- mesons to be isotropic in the overall centre-of-mass frame. This is indeed found to be the case for the background spectrum[39], and any π^0 particles deriving from s-channel resonances show up clearly by having a pronounced production angle.

Fig. 15 displays the background spectra corresponding to various incident pion laboratory momenta, and also the variation of the total cross-section for the background with momentum. This latter behaviour is of interest because it might be expected that the total elastic cross-section for pion-pion scattering would vary in the same manner.

Fig. 16 shows the results of calculations for the related charge mode $\pi^+ p \to \pi^+ \pi^+ n$, comparison with experiment being made at 8 GeV[31].

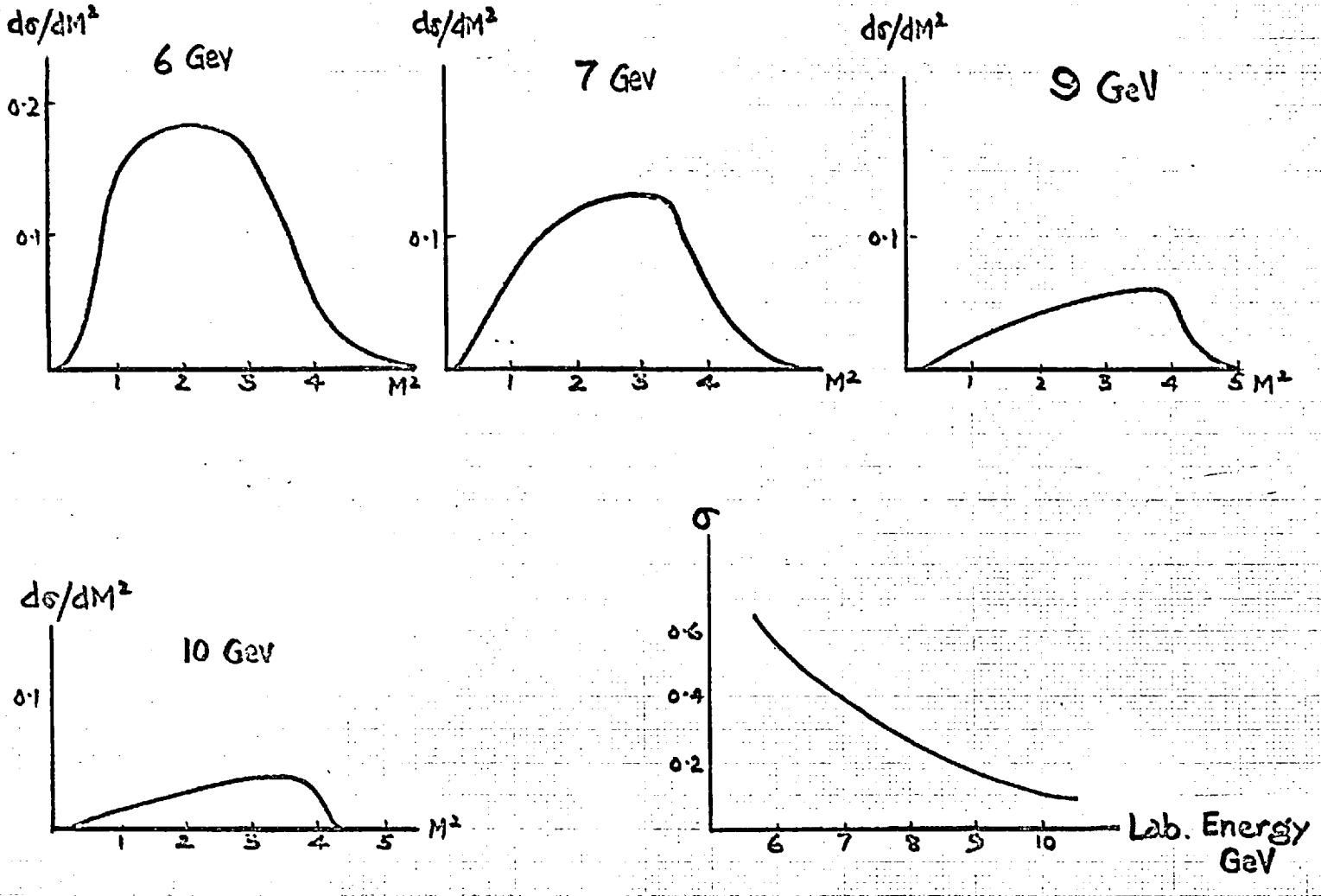

Fig. 15 Energy variation of $\pi^+ p \to \pi^+ \pi^0 p$

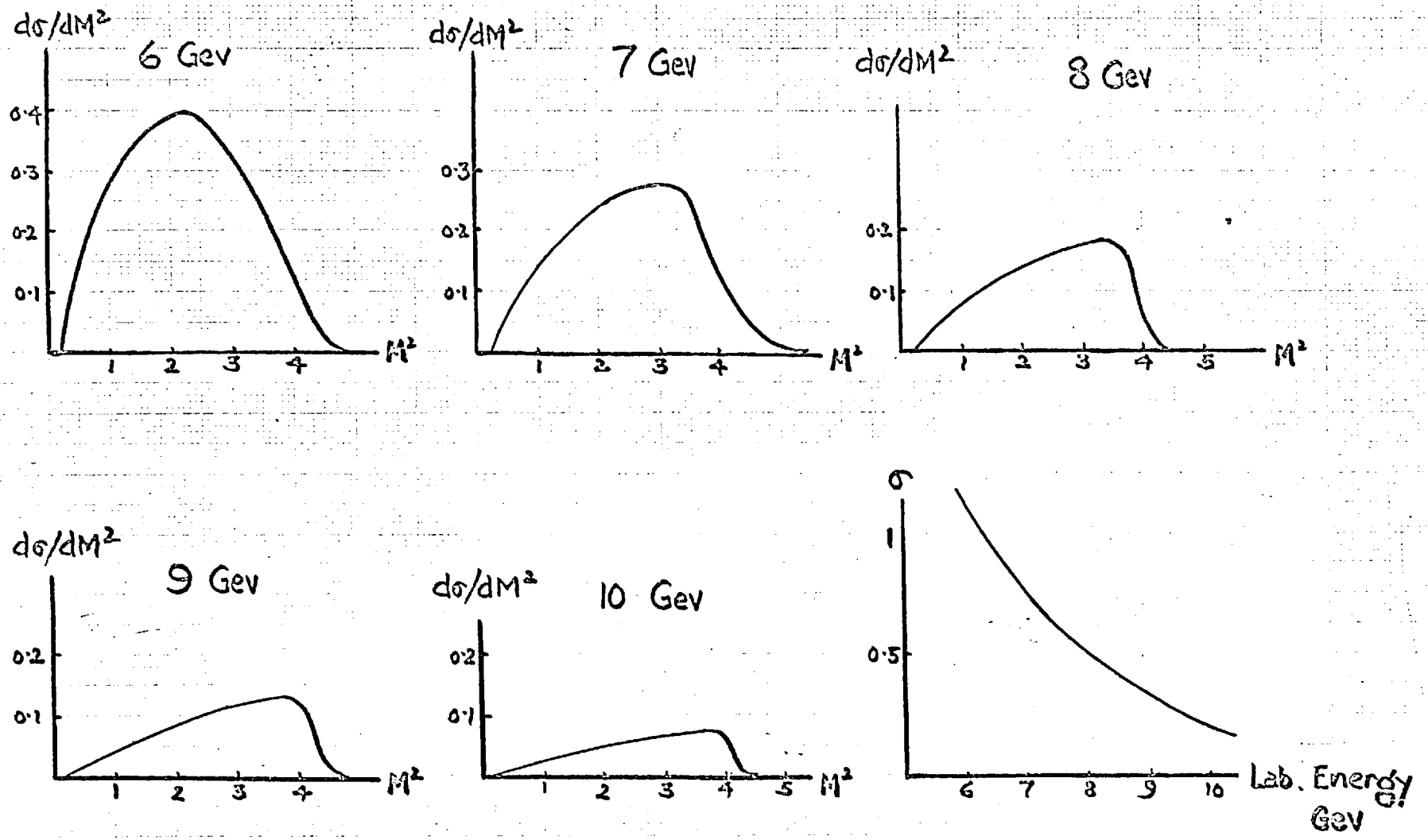

Fig. 16 Energy variation of $\pi^+p \to \pi^+\pi^+n$

Finally it should be mentioned that calculations for these reactions have been carried out[40] assuming that both t-channel poles are Regge poles, rather than writing one pole explicitly as a Feynman term. These calculations yield similar results to those presented here, but are perhaps not capable of an equally graphic visualization. They would correspond to extremely high energy interactions for which pion poles no longer dominate, and where the incident pions interact directly with the nucleon. The produced pions then arise from the overlap of the wave functions of the target nucleons and the projectile mesons.

d) Other Processes

The reaction $\pi N \to \bar{\pi}\pi N$ was eminently suitable for analysis because it could be written in terms of just one amplitude, and so involve a minimum number of adjustable parameters. Other reactions will involve several helicity amplitudes, for instance, the process $NN \to NN\pi$ which can be examined by making the correspondence

$$a \equiv N,\ b \equiv N,\ 1 \equiv N,\ 2 \equiv \pi,\ 3 \equiv N\ .$$

The angular momentum analysis 51 for the crossed channel $N\bar{N} \to N\bar{N}\pi$ becomes

$$T_{\lambda_2'\lambda_3'} = \sum_{\substack{m_1', \nu_3' \\ \nu_2'}} \sum_{i,j} e^{-i\pi s_2} e^{i m_1' \varphi_3'} \frac{\pi}{2\sin\pi(\alpha_{1i}' - \sigma_{1i})} \times \cdots$$

$$\times \left[d_{\lambda_a'-\lambda_b', m_1'}(J_i', \cos\Theta_3') + (-1)^{\sigma_{1i}-\lambda_a'+\lambda_b'} d_{\lambda_a'-\lambda_b', -m_1'}(J_i', -\cos\Theta_3') \right]$$

$$\times \frac{\pi}{2\sin\pi(\alpha_{2j}' - \sigma_{2j})} \left[d_{m_1', \nu_3'-\nu_2'}(j_{ij}', \cos\theta_3') + (-1)^{\sigma_{2j}-m_1'} d_{m_1', -\nu_3'+\nu_2'}(j_{ij}', -\cos\theta_3') \right]$$

$$\times \beta_{ij}(s_{ab}', s_{23}', \lambda') .$$

Assume again that the angular momentum J_i' is represented by a Feynman pion.

$$T_{\lambda_2', \lambda_3'} = \sum_{\nu_3', \nu_2'} \sum_{j} e^{-i\pi s_2} \frac{1}{s_{ab}' - m_\pi^2} \cdot \frac{\pi}{2\sin\pi(\alpha_{2j}' - \sigma_{2j})} \times \cdots$$

$$\times \left[d_{0, \nu_3'-\nu_2'}(j_{ij}', \cos\theta_3') + (-1)^{\sigma_{2j}} d_{0, -\nu_3'+\nu_2'}(j_{ij}', -\cos\theta_3') \right] \beta_{ij}(s_{ab}', s_{23}', \lambda') .$$

There are two amplitudes, namely $T'_{1/2, 1/2}$ and $T'_{1/2, -1/2}$ each of which possesses its own set of residues, $\beta_{ij}(\lambda)$.

Before dealing with so many free parameters, it might be instructive to neglect spin in order to determine the general features of the model. A complete treatment with spin can be considered as adding some additional fine structure to the scalar behaviour. So write a

scalar amplitude :

$$T' = \frac{g_{NN\pi}}{s'_{ab} - m_\pi^2} \sum_i \frac{\pi \beta_i(s'_{23})}{2 \sin \pi(\alpha_i' - \sigma_i)} \left[1 + e^{-i\pi(\alpha_i' - \sigma_i)}\right] \left(\frac{\cos \theta'_3}{2}\right)^{\alpha_i'}$$

In the direct channel the twin poles must necessarily be of opposing G-parities, but these parities are not fixed absolutely. In physical language this means that the liberated pion can emanate either from the target nucleon or the projectile nucleon, these being indistinguishable in the overall centre-of-mass frame. It must also be remembered when calculating a πN final state mass-spectrum that there are in fact two πN sub-systems in the final state which are experimentally indistinguishable. This is taken into account by taking an average matrix element from the two diagrams shown in Fig. 17 and evaluating the resulting mass-spectrum from the (12) subsystem. These diagrams can be obtained from

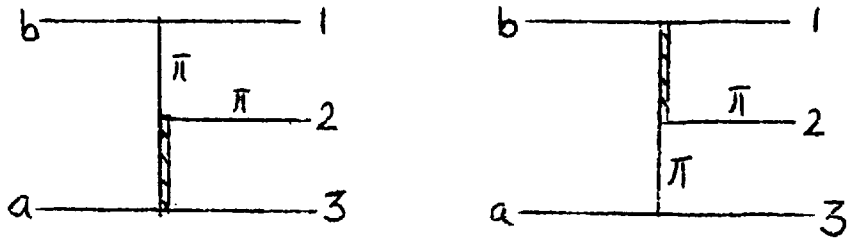

Fig. 17 Indistinguishability in $NN \to NN\pi$
The thick lines denote positive - G Regge trajectories

each other simply by reversing the order of the particle labels so that there occurs an interchange of S_{12} and S_{23}, and also of t_{3a} and t_{1b}.

There now arises the problem of the free parameters in the vertex functions. The reaction $NN \to NN\pi^0$ can have no contribution from a ρ-Regge pole, the elastic scattering being due entirely to the two Pomeranchuk poles with the quantum numbers of the vacuum.

It was hoped at first that the parameterizations for this process could be fixed by previous analyses of pion-nucleon elastic scattering data[5], but this hope was in vain. This was because the angular dependence $\left(\frac{\cos\theta'_3}{2}\right)^{\alpha_i}$ was represented for the two-particle scatterings by a particularly simple form S^{α_i}, obtained by employing the asymptotic form 6. This form is not suitable for use in a three-particle final state, the expression 21 showing that even at high energy the scattering angle has a detailed structure. This data still provides, however, the exponential parameters C_{ii} and the ratio $C_{0P}/C_{0P'}$, so that only an overall scale factor remains which does not affect in any way the actual behaviour of the calculated mass spectrum.

The results of the calculation are shown in Fig. 18 for

proton energies of 8, 12 and 15 GeV, and show some very interesting properties. As for the case $\pi N \to \pi\pi N$, the mass spectra are confined to the lower mass values, and fall to a low minimum value well before the phase space limit is attained. This means again that the central region of the experimental Dalitz plot should not show a uniform population. Since essentially two matrix elements are calculated, it might be hoped that provided the interference between them is not too large, the final results will show two distinct patterns of behaviour. If the final pion emanates from a projectile nucleon, then the pattern of events will be roughly characteristic of free pions scattering from target nucleons, whereas a pion from a target nucleon will show an effect very much that which would be expected from nucleons scattering from target pions. This latter process would have a very low effective centre-of-mass energy, and and thus accounts for the large enhancement for very low effective masses, the remainder of the spectrum being due to pion-on-nucleon and interference effects.

These low-mass enhancements are much more pronounced than any others which have been calculated so far, but their width of several GeV units is much too broad for these phenomena to be mistaken by a sane experimentalist for a resonance. The existence

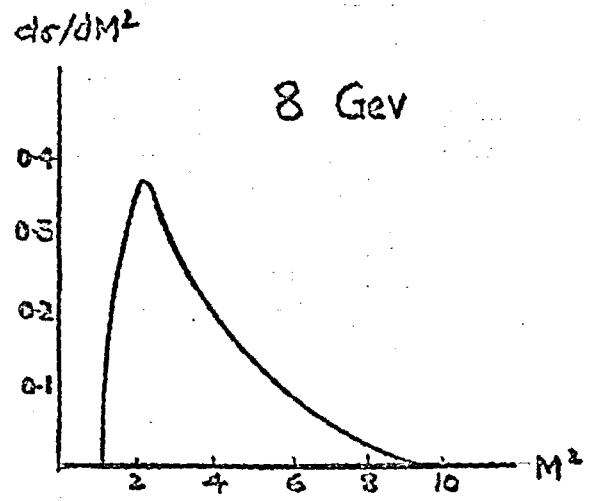

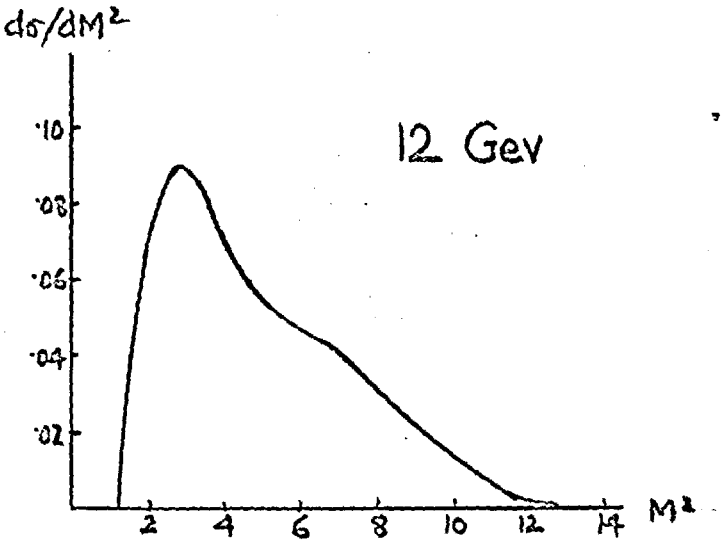

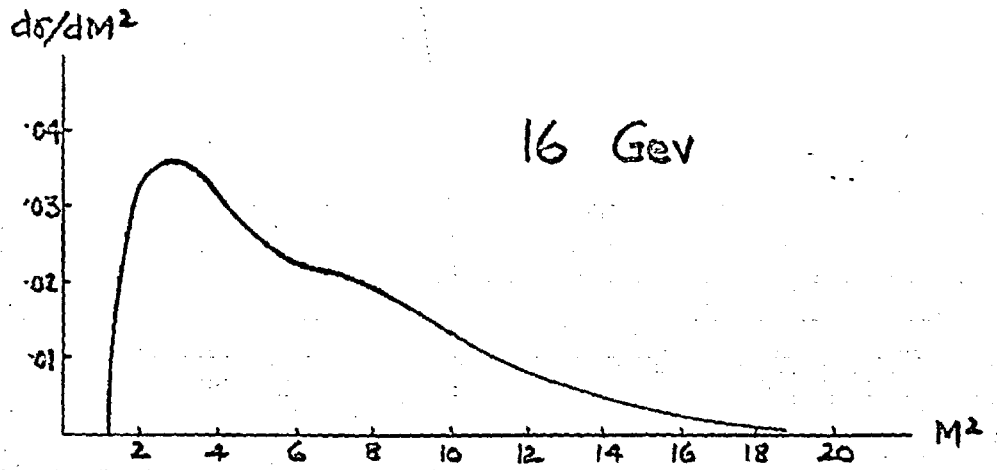

Fig. 18

Energy variation of $pp \to pp\pi^0$

of such enhancements in a region which is already plentiful with nucleon resonances could have nevertheless serious implications due to interference effects.

Most of the nucleon resonances display a differential cross-section $d\sigma/dt$ which when parametrized by a form Ae^{bt} require a value for b which lies in the range 4 GeV to 7 GeV. Two notable exceptions to this rule are the $N^*_{3/2,3/2}$ (1238) and the N* (1400) which are only fitted if b lies in the range 15 GeV to 20 GeV[41]. It is interesting to conjecture that this could be due to interference between the amplitudes for resonance production and the backg round. Experimentally the various nucleon resonances manifest themselves by a characteristic behaviour of pion-nucleon two-particle subsystems in the final state and are readily selected out. There is very little that can be done to this data to eliminate the effects of interference between the amplitude for resonance production and the background spectrum, if the exact form of the background spectrum is not known.

It should be possible in theory to write matrix elements for the $NN \to NN\pi$ production process by employing directly the amplitudes for pion-nucleon scattering which are free from kinematical singularities. Such a matrix element would take the form

$$|T|^2 = \frac{g^2_{NN\pi}}{2}\left[\frac{1}{(t_{3a}-m_\pi^2)^2}\left(|F_{++}(t_{1b})|^2+|F_{+-}(t_{1b})|^2\right)\right.$$

$$\left.+\frac{1}{(t_{1b}-m_\pi^2)^2}\left(|F_{++}(t_{3a})|^2+|F_{+-}(t_{3a})|^2\right)\right]$$

Where F_{++} and F_{+-} are the amplitudes for no-flip and flip pion-nucleon scattering, respectively. This would demand that the angular dependence in these amplitudes would have to be kept explicitly in the form $\left(\frac{\cos\theta_{3t}}{2}\right)^{\alpha_i}$ with a minimum of asymptotic expressions being introduced. It is perhaps a pity that the current forms for the pion-nucleon amplitudes have approximated the crossed-channel angular dependence by the particularly simple expression E^{α_i} where E is the incident pion laboratory energy. Such an expression is highly unsatisfactory for use with pion propagator terms.

e) Regge Residues

Any formulation of a high-energy scattering amplitude using complex angular momentum techniques has the drawback that the explicit couplings of the external particles to the exchanged Regge trajectories are completely undetermined by any theoretical argument.

It has recently been suggested that these vertex coupling strengths could be governed by algebraic principles[42]. The idea was that the vertex functions for fixed momentum transfer would appear as operators of a homogeneous $\mathcal{U}(12)$ algebra, and the coupling strengths would be obtained by taking matrix elements of these operators in some way. It is obviously convenient to choose the fixed momentum transfer at zero, and so set up a formalism for two-particle forward scattering amplitudes, which can then be related into terms of total cross-sections using the optical theorem. The factorization hypothesis for the Regge couplings is tacitly assumed, and furthermore, the idea of an effective quark model is used, so that the total residue for a particular two-particle scattering process $A + B \rightarrow C + D$ in the forward direction comes out as

$$G = \sum_{Q} G(ABR)G(CDR)$$

where G(ABR) represents the coupling of the quarks in A and B to the Regge trajectories and $\sum_{Q}'$ denotes a sum over all quark combinations. Thus the model assumes that exchange mechanisms occur between quark pairs, and the observable effect is obtained by adding all possible such contributions.

The extreme high-energy behaviour is said to be due to a set of coupling strengths S^i constructed in such a way as to be the

same for quark-quark or quark-antiquark couplings to Regge poles.

$$S^i = \int d^3x\, q_1^\dagger \beta \lambda^i q_2$$

The set S^i transforms as a nonet, and the matrix β renders the particle/antiparticle nature of the participating quarks immaterial. In this way the model is made compatible with the Pomeranchuk theorem. The systematic deviation away from the Pomeranchuck behaviour is credited to a second nonet of strengths V^i.

$$V^i = \int d^3x\, q_1^\dagger \lambda^i q_2$$

These strengths now differentiate between quark-quark and quark-antiquark couplings to provide, for example, a difference between proton-proton and proton-antiproton total cross-sections. It is hoped that such a $U(3) \otimes U(3)$ algebra is sufficient to describe the coupling strengths for non-spin flip forward scattering. The introduction of spin flip would necessitate enlarging the algebra to cover $U(6) \otimes U(6)$. For use with the optical theorem, however, only non-flip terms are needed.

For elastic scattering, only the diagonal forms contribute, viz S^0, S^3, S^8, V^0, V^3 and V^8. S^0 and S^8 are identified with the two Pomeranchuk contributions, S^3 with the R (A2) trajectory, V^0 and V^8 with ω and φ, and V^3 with the ρ.

A simple example of this scheme is the derivation of the Levin-Frankfurt ratio for the total cross-sections of pion-proton and proton-proton scatterings at high energy[43), 1)]. Restricting to the energy region where only Pomeranchuk contributions are important,

$$\frac{\sigma_{\pi p}}{\sigma_{pp}} = \frac{\sum' [S^0(\pi\pi) + S^8(\pi\pi)][S^0(pp) + S^8(pp)]}{\sum_Q [S^0(pp) + S^8(pp)][S^0(pp) + S^8(pp)]} = \frac{2}{3} .$$

This is in fair agreement with experiment. With this success in mind, a similar ratio should exist relating the residues for pion-pion and pion-nucleon forward scattering amplitudes,

$$\frac{A_0(\pi\pi)}{A_0(\pi p)} = \frac{\sum' [S^0(\pi\pi) + S^8(\pi\pi)][S^0(\pi\pi) + S^8(\pi\pi)]}{\sum_Q [S^0(\pi\pi) + S^8(\pi\pi)][S^0(pp) + S^8(pp)]} = \frac{2}{3} .$$

This prediction seems woefully inadequate, since it was demonstrated in part 2 how pion-pion elastic couplings are down by a factor of ten on the pion-nucleon ones. This phenomenon should manifest itself when comparing the Regge residues used in the calculations for $\pi N \to \pi\pi N$ and $NN \to NN\pi$. Unfortunately the precise background spectrum for the latter reactions is difficult to measure due to the vast number of nucleon resonances seen in the final state. The reaction $Kp \to K^*\pi p$ requires a knowledge of pion-

nucleon scattering amplitudes to calculate its background spectrum (see Fig. 15). Calculations show that the residues needed to obtain agreement with experiment are indeed up by a significant factor on those for the pion-pion part in $\pi N \to \pi\pi N$ [44].

Comparison with Other Work and Final Conclusions

The initial works on particle production via virtual diffraction scattering[27] were of the firm opinion that some observed resonance effects were due to the kinematical diffraction mechanism. Recent work[45] has suggested that some higher nucleon resonances might be accounted for by this same effect. It is very difficult to reconcile the claims of these workers with the conclusions drawn from Part Two of this thesis. But a recent article[46] seems to indicate that more extensive calculations have caused people to change their minds. It now seems that they too believe how diffraction and dissociation contribute to a characteristic background spectrum for production processes, and that some knowledge of this spectrum is necessary in order to isolate the true resonance behaviour. There was a great temptation to always assign a simple phase-space distribution of constant matrix-element to the background, with the result that the statistics presented for resonance production would always display some effects that in fact were due to the true background.

The work so far has been confined mainly to invariant mass distributions, since these plots are equally accessible to both measurement and calculation, but there is an urgent demand for calculations

on, for instance, the various angular distributions of the final particles. For this purpose the usual method of using the phenomenological four-point diffraction vertex is highly unsuitable, since it is parametrized in a very naive manner. It predicts an isotropic distribution for all Treiman-Yang angles which is not obtained in practice. A more sophisticated model is called for, and the multiperipheral mechanism is an attempt to provide this.

The multiperipheral model gives essentially the same results as the old Drell-Deck diffraction mechanism and can be considered to supersede it, but with the knowledge that it is really the background spectrum for which it is responsible. Meaningful calculations on angular distributions are now possible.

There is perhaps some doubt as to which poles should in fact be employed in a multiperipheral model. This work has used a Regge pole and a particle pole together, whereas other workers[40] have employed only Regge poles. Each of these procedures probably has an energy range where its application is justified, just as in the case of two-particle scatterings. But the general features of the model are to a certain extent independent of the choice of poles.

REFERENCES

1). K. Johnson, S. B. Treiman; Phys. Rev. Letters 14, 189 (1965) R. Sawyer; Phys. Rev. Letters 14, 471 (1965)

2). See for example the lectures by J. J. J. Kokkedee at VI Universitatswochen fur Kernphysik, Schladming. CERN preprint 67/163/5 - TH. 745
H. J. Lipkin, F. Scheck; Phys. Rev. Letters 16, 71 (1966)
H. J. Lipkin; Phys. Rev. Letters 16, 1015 (1966)

3). E. Ferrari, F. Selleri; Supp. d. Nuo. Cim 24, 453 (1962). Nuo. Cim. 27, 1450 (1963), Phys. Rev. Letters 3, 76 (1961)
F. Bonsignori, F. Selleri; Nuo. Cim. 15 465 (1960)
S. D. Drell; Phys. Rev. Letters 5, 278, 342 (1960)
F. Salzman, G. Salzman; Phys. Rev. Letters 5, 377 (1960)
Phys. Rev. 120, 599 (1960), 121, 1541 (1961)
E. Clementel, C. Villi; Nuo. Cim. 4, 1207 (1956)
U. Amaldi, F. Selleri; Nuo. Cim. 31, 360 (1964)
J. D. Jackson, H. Pilkuhn; Nuo. Cim. 33, 906 (1964)

4). T. Regge; Nuo. Cim. 14, 951 (1959); 18, 947 (1960)
G. F. Chew, S. C. Frautschi; Phys. Rev. Letters 7, 394 (1961)
S. C. Frautschi, M. Gell-Mann, F. Azchariasen; Phys. Rev. 126, 2204 (1962)
V. N. Gribov; Soviet Physics JETP 14, 478 (1962)

5). R. J. N. Phillips, W. Rarita; Phys. Rev. 139, B1336, 138, B723, (1965)
A. Pignotti; Phys. Rev. 134, B630 (1964)
A. Ahmadzadeh; Phys. Rev. 134, B633 (1964)

6). K. Gottfried, J. D. Jackson; Nuo. Cim. 33, 309 (1964)

7). J. J. Sakurai; Vector Mesons and Unitarity Symmetry in 'Theoretical Physics' published by IAEA, Vienna 1963.

8). A. Salam, R. Delbourgo, J. Strathdee; Proc. Roy. Soc. A284, 146 (1965)
B. Sakita, K. C. Wali; Phys. Rev. 139, B1355 (1965)
M. A. B. Beg, A. Pais,; Phys. Rev. Letters 14, 267 (1965)

9). N. J. Sopkovitch; Nuo. Cim. 26, 186, (1962)
L. Durand, Y. T. Chiu; Phys. Rev. Letters 12, 399 (1964)
Phys. Rev. 137, B1530 (1965), ibid 139, B646 (1965)
K. Gottfried, J. D. Jackson; Neo. Cim. 34, 735 (1964)
J. D. Jackson; Rev. Mod. Phys. 37, 484 (1965)

10) J.H.R. Migneron, H.D.D. Watson; Phys. Letters 19, 424 (1965), and Imperial College preprint ICTP 67/7 , submitted to Phys. Rev. J.H.R. Migneron, K. Moriarty; Imperial College preprint ICTP 67/10 , submitted to Phys. Rev. Letters

11) D.E. Damouth, L.W. Jones, M.L. Perl; Phys. Rev. Letters 11, 287 (1963) R. Crittenden, H.J. Martin, W. Kernan, L. Leipner, A.C. Li, F. Ayer, L. Marshall, M.L. Stevenson; Phys. Rev. Letters 12, 429 (1964)
M.N. Focacci, S. Focardi, G. Giacomelli, P. Serra, M.P. Zerbetto, L. Monari; Phys. Letters 19, 441 (1965)
K.J. Foley, S.J. Lindenbaum, W.A. Love, S. Ozaki, J.J. Russell, L.C.L. Yuan; Phys. Rev. Letters 11, 503 (1963)

12) Notably by V. Singh; Phys. Rev. 129, 1889 (1963)
W.R. Frazer, J. Fulco; Phys. Rev. 117, 1603 (1960)
V. Barger, M. Ebel; Phys. Rev. 138, B1148 (1965)

13) H. Högaasen, J. Högaasen; Nuo. Cim. 39, 941 (1965)
K.E. Lassila; Nuo. Cim. 42, 403 (1966)

14) R.K. Logan; Phys. Rev. Letters 14, 414 (1965)
R.J.N. Phillips, W. Rarita; Phys. Rev. 139, B1336

15) V. Barger, D. Cline; Phys. Rev. Letters 16, 913 (1966)

16) H. Högaasen, W. Fischer; Phys. Letters 22, 516 (1966)

17) J.D. Jackson, J.T. Donohue, K. Gottfried, R. Keyser, B.E.Y. Svensson; Phys. Rev. 139, B428 (1965)
B.E.Y. Svensson; Nuo. Cim. 37, 714; 39, 66 (1965)
L. Durand, Y.T. Chiu; Phys. Rev. 137, B1530 (1965)
G.A. Ringland, R.J.N. Phillips; Phys. Letters 12, 62 (1964)
Aachen - Berlin - Birmingham - Bonn - Hamburg - London - München collaboration; Nuo. Cim. 35, 659 (1965)

18) M. Ferro-Luzzi, R. George, Y. Goldschmidt-Clermont, V.P. Henri, B. Jongejans; Proceedings of 1963 Sienna International Conference on Elementary Particles, Vol. I
G.R. Lynch, M. Ferro-Luzzi, R. George, Y. Goldschmidt-Clermont, V.P. Henri; Phys. Letters 9, 359 (1964)
J.D. Jackson; Rev. Mod. Phys. 37, 484 (1965)

19) H.D.D. Watson, Phys. Letters 17, 72 (1965)

20) R.H. Dalitz; 'Strange Particles and Strong Interactions', Oxford 1962

21) G. Fraser; Phys. Letters 19, 521 (1965)
P. R. Graves-Morris; Ann. Phys. 41, 477 (1967)
H. Pilkuhn; Lectures at V. Universitätswochen für Kernphysik, Schladming, published in Acta Physica Austriaca 1966.
P. T. Matthews, A. Salam, Nuovo Cimento 13, 381 (1959)

22) T. W. B. Kibble; Phys. Rev. 131, 2282 (1963)

23) G. F. Chew, F. E. Low; Phys. Rev. 113, 1640 (1959)
C. Goebel; Phys. Rev. Letters 1, 337 (1958)
E. Pickup, D. K. Robinson, E. O. Salant; Phys. Rev. Letters 7, 192 (1962)

24) G. C. Wick; Ann. Phys. 18, 65 (1962)

25) M. S. K. Razmi; Nuo. Cim. 31, 615 (1964)

26) S. D. Drell, K. Hiida; Phys. Rev. Letters 7, 199 (1961)

27) R. T. Deck; Phys. Rev. Letters 13, 169 (1964)
U. Maor, T. A. O'Halloran; Phys. Letters 15, 281 (1965)

28) A. H. Rosenfeld; Proc. Oxford Int. Conf. (1965)

29) P. K. Chaudhuri; Private communication from Birmingham, Glasgow, London, Munich, Oxford, Rutherford Laboratory collaboration (1966)

30) Preliminary data from the Aachen, Berlin, CERN, London, Vienna collaboration (1966)

31) M. Deutschmann, R. Schulte, H. Weber, W. Woisching, C. Grote, J. Klugow, S. Nowak, S. Brandt, V. T. Cocconi, O. Czyzewski, P. F. Dalpiaz, G. Kellner, D. R. O. Morrison, Phys. Letters 12, 356 (1964)

32) M. Deutschmann, R. Schulta, R. Steinberg, H. Weber, W. Woisching, C. Grote, J. Klugow, W. Meyer, S. Nowak, S. Brandt, V. T. Cocconi, O. Czyzewski, P. F. Dalpiaz, E. Flaminio, G. Kellner, D. R. O. Morrison; Phys. Letters 18, 351 (1965)

33) G. Fraser, R. G. Roberts; Nuo. Cim. 47, 293 (1967)

34) J. D. Jackson; Rev. Mod. Phys. 37, 484 (1965)
L. Van Hove; Int. Conf. Berkeley (1966)

35) T. W. B. Kibble; Phys. Rev. 117, 1159 (1960)
D. A. Atkinson, V. Barger; Nuo. Cim. 38, 634 (1965)

36) J.M. Charap, E.J. Squires; Ann. Phys. 20, 145 (1965)

37) T.L. Trueman, G.C. Wick; Ann. Phys. 26, 322 (1964)

38) R.G. Roberts, G. Fraser, Durham preprint 1967, to be published in Physical Review

39) Aachen, Birmingham, Bonn, Hamburg, London, München collaboration, Nuo. Cim. 31, 729 (1964)

40) Chan Hong-Mo, K. Kajantie, G. Ranft; CERN preprint 66/1260/5 - TH. 719

41) E.W. Anderson, E.J. Bleser, G.B. Collins, T. Fujii, J. Menes, F. Turkot, R.A. Carrigan, R.M. Edelstein, N.C. Hien, T.J. McMahon, I. Nadelhaft; Phys. Rev. Letters 16, 855 (1966)

42) N. Cabibbo, L. Horwitz, Y. Ne'eman; Phys. Letters 22, 336 (1966).

43) E.M. Levin, L.L. Frankfurt; Zh. Eksp. i. Teor Fiz. Pizma v. Redak. 2, 105 (1965), JETP Letters 2, 65 (1965)

44) J.L. Schonfelder; Private communication (1967)

45) L. Resnick; Phys. Rev. 150, 1292 (1966)

46) U. Maor; Ann. Phys. 41, 456 (1967)

Reprinted from

PHYSICS LETTERS

Volume 19, number 6, 1 December 1965

MASS SPLITTING AND UNITARITY

G. FRASER

pp. 521 - 523

NORTH-HOLLAND PUBLISHING COMPANY

AMSTERDAM

MASS SPLITTING AND UNITARITY *

G. FRASER
Physics Department, Imperial College, London S.W.7

Received 5 November 1965

Recently several authors have calculated ratios of amplitudes for various proton-antiproton annihilation modes at rest on the basis of a broken inhomogeneous $\bar{U}(12)$ symmetry scheme [1]. Their results are in serious disagreement with experiment. Their calculations neglect mass splitting within the baryon octet. Although the mass-splitting between the observed particles is small, the splitting within the baryon octet is large. For stopped $p\bar{p}$ reactions, this suppresses intermediate states composed of behaviour baryon-antibaryon pairs. This will have an effect on the observed process because of unitarity. This note presents a method for estimating these effects using the inverse reaction matrix formalism of Matthews and Salam [2].

The following model is an excellent illustration of the approach. For $p\bar{p}$ reactions consider only the nucleon and K-meson states and allow for an arbitrarily large p-n mass difference, all other masses being degenerate. Label the channels as follows:

$1 \equiv p\bar{p}, \quad 2 \equiv K^+K^-, \quad 3 \equiv K^0\bar{K}^0, \quad 4 \equiv n\bar{n}.$

* The research reported in this document has been sponsored in part by the Air Force Office of Scientific Research OAR through the European Office of Aerospace Research, United States Air Force.

Time reversal makes T^{-1} symmetric. Define $\overline{T}_{ij}^{-1}$ as that matrix which describes nucleon-antinucleon scattering at rest in this scheme with all the masses in the baryon octet degenerate and T_{ij}^{-1} as the matrix which describes proton-antiproton scattering at rest with the one mass split between proton and neutron. Set $T^{-1} = \overline{T}^{-1} + \Delta$ so that $T = \overline{T}(1 + \Delta\overline{T})^{-1}$.

The approach of Matthews and Salam [2] enables the mass-splitting matrix Δ to be written as

$$\Delta = \begin{pmatrix} 0 & 0 & 0 & 0 \\ 0 & 0 & 0 & 0 \\ 0 & 0 & 0 & 0 \\ 0 & 0 & 0 & \delta \end{pmatrix}$$

where δ is the magnitude of the 3-momentum in the c.m. frame corresponding to the observed mass-split, Δm. This gives the following amplitudes:

$$T_{22} = \overline{T}_{22} - \frac{\delta\overline{T}_{24}\,\overline{T}_{24}}{1 + \delta\overline{T}_{44}}$$

$$T_{33} = \overline{T}_{33} - \frac{\delta\overline{T}_{34}\,\overline{T}_{34}}{1 + \delta\overline{T}_{44}}$$

An i-spin analysis of the K-particle submatrix

$$\begin{pmatrix} \overline{T}_{22} & \overline{T}_{23} \\ \overline{T}_{23} & \overline{T}_{33} \end{pmatrix}$$

gives $\overline{T}_{22} = \overline{T}_{33}$

Thus

$$\frac{T_{22}}{T_{33}} = \frac{\overline{T}_{22}(1 + \delta\overline{T}_{44}) - \delta\overline{T}_{24}^{\,2}}{\overline{T}_{22}(1 + \delta\overline{T}_{44}) - \delta\overline{T}_{34}^{\,2}}$$

Following Hussain and Rotelli [1], a $\tilde{U}(12)$ estimation of the amplitudes for $n\bar{n} \to K^+K^-$, $n\bar{n} \to K^0\bar{K}^0$ gives

$$\frac{\overline{T}_{34}}{\overline{T}_{24}} = \frac{2}{1}$$

so that

$$\frac{T_{22}}{T_{33}} = \frac{\overline{T}_{22}(1 + \delta\overline{T}_{44}) - \delta\overline{T}_{24}^{\,2}}{\overline{T}_{22}(1 + \delta\overline{T}_{44}) - 4\delta\overline{T}_{24}^{\,2}}$$

which is greater than unity.

This demonstrates the effect of below threshold intermediate states on the i-spin relations between physical amplitudes. Suppose $\delta \to \infty$.

This means that the $n\bar{n}$ channel is no longer available as an intermediate state and all traces of nucleon i-spin are lost. For this case

$$\frac{T_{22}}{T_{33}} \to \frac{\overline{T}_{22}\overline{T}_{44} - \overline{T}_{24}^{\,2}}{\overline{T}_{22}\overline{T}_{44} - 4\overline{T}_{24}^{\,2}}\,.$$

If the T-matrix elements are expressed in terms of T^{-1} matrix elements by direct matrix inversion, then this final relation is found to be precisely that which would be obtained by inverting a T^{-1} matrix involving channels 1, 2 and 3 only.

Apply this now to a more realistic model for stopped $p\bar{p}$-annihilation into K-mesons. Re-label the channels as

$1 \equiv p\bar{p}$, $\quad 2 \equiv K^+K^-$, $\quad 3 \equiv K^0\bar{K}^0$, $\quad 4 \equiv$ "$\Xi\bar{\Xi}$".

The "Ξ" particle used here represents the combined effect of all below threshold intermediate baryon states. This trick enables the mass-splitting to be accounted for by just one channel. Hussain and Rotelli's work [1] enables the following ratios of amplitudes to be obtained:

$$\frac{p\bar{p} \to K^+K^-}{p\bar{p} \to K^0\bar{K}^0} = \frac{2}{1} \qquad \frac{\bar{\Xi}^0\Xi^0 \to K^+K^-}{\bar{\Xi}^0\Xi^0 \to K^0\bar{K}^0} = \frac{-1}{-2}$$

$$\frac{n\bar{n} \to K^+K^-}{n\bar{n} \to K^0\bar{K}^0} = \frac{1}{2} \qquad \frac{\bar{\Xi}^-\Xi^- \to K^+K^-}{\bar{\Xi}^-\Xi^- \to K^0\bar{K}^0} = \frac{-2}{-1}$$

$$\frac{\bar{\Sigma}^+\Sigma^+ \to K^+K^-}{\bar{\Sigma}^+\Sigma^+ \to K^0\bar{K}^0} = \frac{1}{-1} \qquad \frac{\bar{\Sigma}^-\Sigma^- \to K^+K^-}{\bar{\Sigma}^-\Sigma^- \to K^0\bar{K}^0} = \frac{-1}{1}$$

No amplitudes are obtained for the decay of $\bar{\Sigma}^0\Sigma^0$ or $\bar{\Lambda}^0\Lambda^0$ into 2 K-particles. Notice that the amplitudes for the heavier baryons are negative whilst those for the light baryons are positive. Retain all these negative signs so that different amplitudes can be compared. Write amplitudes for the representative "Ξ"-particle so that

$$\frac{\overline{T}_{24}}{\overline{T}_{34}} = \frac{-1}{-1}\,.$$

This gives

$$\frac{T_{12}}{T_{13}} = \frac{2\overline{T}_{13}(1 + \delta\overline{T}_{44}) + \delta\overline{T}_{14}\,|\overline{T}_{24}|}{\overline{T}_{13}(1 + \delta\overline{T}_{44}) + \delta\overline{T}_{14}\,|\overline{T}_{24}|}$$

$$= \frac{2 + 2\delta\overline{T}_{44} + \delta\overline{T}_{14}\,|\overline{T}_{24}|/\overline{T}_{13}}{1 + \delta\overline{T}_{44} + \delta\overline{T}_{14}\,|\overline{T}_{24}|/\overline{T}_{13}}\,.$$

Because of kinematical factors in the amplitudes, $|\overline{T}_{24}|/\overline{T}_{13} \doteqdot 1.4$. Information from $p\bar{p}$ experiments [3] at these energies gives the ratio of amplitudes

$$\frac{p\bar{p} \to p\bar{p}}{p\bar{p} \to n\bar{n}} \doteqdot 2.5 \ .$$

Assuming that $\overline{T}_{44}/\overline{T}_{14}$ is near this value, then

$$\frac{T_{12}}{T_{13}} \doteqdot 2 - \frac{2.5\delta}{1/\overline{T}_{14} + 3.9\delta},$$

which is estimated at 1.4, and is not very sensitive, the important point being that $\delta \gg \overline{T}_{14}^{-1}$. This compares favourably with the latest experiments, which give [4]

$$\frac{T_{12}}{T_{13}} = 1.34.$$

In general the corrected amplitude assuming one intermediate state below threshold can be written as

$$T_{ij} = \overline{T}_{ij} - \frac{\delta \overline{T}_{in} \overline{T}_{jn}}{1 + \delta \overline{T}_{nn}},$$

where $\overline{T}$ is the reaction matrix assuming degenerate masses and where relations between amplitudes have been established using group theory. Also i,j and n are channel labels, n being the below threshold particle combination.

I wish to thank Professor P. T. Matthews for suggesting this problem and for many profitable discussions.

References

1. F. Hussain and P. Rotelli, Physics Letters 16 (1965) 183. Imperial College preprint ICTP/65/28; P. Winternitz et al., Dubna preprint 1965; L. Schülke, Heidelberg preprint 1965; Chai S. Lai, Phys. Rev. Letters 15 (1965) 563.
2. P. T. Matthews and A. Salam, Nuovo Cimento 13 (1959) 381.
3. E. Segre in Nobel lectures 1942-1962 (Elsevier 1964) p. 513.
4. Baltay, Barash et al., Phys. Rev. Letters 15 (1965) 532.

* * * * *